

Representing inhibition in growth kinetics: the Haldane KIS

Nan PAN¹, Liu-Di LU^{2*}, Olivier BERNARD^{3, 4},

1 LIX, CNRS UMR 7161, École Polytechnique, Institut Polytechnique de Paris, Palaiseau, France

2 Section of Mathematics, University of Geneva, Geneva, Switzerland

3 INRIA Centre d'Université Côte d'Azur, BIOCORE Project-Team, Université Nice Côte d'Azur, Sophia-Antipolis Cedex, France

4 Sorbonne Université, CNRS, Laboratoire d'Océanographie de Villefranche, Villefranche-sur-mer, France

Abstract

This article focuses on the practical application of the Haldane model to study microbial growth, a critical aspect in various industrial and environmental contexts. We examined four existing parameterizations of the Haldane model in the literature and introduced an additional parameterization based on only two parameters. We investigated the interrelations among these five parameterizations in the context of photoinhibited microalgae growth rate. Using a state-of-the-art model identification technique, we performed sensitivity analyses on each parameter in all parameterizations. Furthermore, we introduced a novel criterion to account for the model accuracy in the selection of the most suitable parameterization of one same model.

Using experimental data on the response of microalgal growth to irradiance, we determined the parameter values for each parameterization and for each data set. The correlation between each parameter is discussed. When parameters within a parameterization exhibit strong correlations, they convey similar information, rendering the parameterization less efficient. Sensitivity analysis, combined with an upgrade of the Akaike information criterion (AIC_c) and the Bayesian information criterion (BIC), identified our two-parameter parameterization as the optimal choice for representing microalgae growth rate in response to irradiance variations. Importantly, the novel information criterion, namely PEMAC, outperforms traditional criteria such as AIC_c and BIC in distinguishing between equivalent parameterizations. This work illustrates the hidden complexity in inhibition models and ends up with a wise recommendation for the modelling of inhibition: *Keep It Simple (KIS)*.

Introduction

Microorganisms, such as bacteria, cyanobacteria, microalgae, or yeast, have tremendous potential for a wide range of applications. Due to their simple cellular structure, they can be grown quickly and efficiently in bioreactors, for pollution removal, feed or food production, and for the production of high value-added products in the chemical industry [1–4]. Additionally, various microorganisms offer avenues for the production of biofuels, using their potential to store lipids and carbohydrates that can be converted to biodiesel and ethanol [5–7]. Photosynthetic microorganisms (cyanobacteria and microalgae) can even contribute to the fixation of CO_2 and its transformation into valuable products for green chemistry or for the production of biofuels [8]. A common

problem for many of these applications is the drop in process efficiency when one of the compounds, typically a substrate, is in excess and becomes an inhibitor, such as for ammonium [9], sodium [10], light [11] or phenol [12]. Models that support advanced control strategies can be the cornerstone of better managing inhibition [13, 14]. However, the models that represent growth at low concentration and then inhibition present some technical issues that make their calibration difficult, and this is the main focus of this paper.

There exists a broad range of mathematical models that can represent the growth kinetics of microorganisms as a function of the main factors affecting their metabolism. We refer to [15] for a brief review of some widely used models. Among them, the Monod model, introduced by J. Monod in [16], is probably the most famous kinetic model due to its simple formula and its ability to represent substrate-limited microbial growth [17, 18]. However, as J.F. Andrews later pointed out in [19]:

..., the Monod relationship cannot be valid for those substrates which limit
growth at low concentrations and are inhibitory to the organism at higher
concentrations.

To account for inhibition at high substrate concentrations, Andrews proposed in [19] the use of the Haldane model [20], initially developed by J.B.S. Haldane to represent enzymes inhibition by high substrate concentrations, to describe the microbial growth kinetics. In particular, it was noted:

Although there is no theoretical basis for the use of this function for
microorganisms, it should be pointed out that the Monod relationship,
which is empirical, is similar in form to the Michaelis-Menton expression
upon which the Haldane function is based.

Since then, the Haldane model has become one of the most popular approaches to represent substrate inhibition in microbial growth kinetics. It shows a reasonable fit to experimental data for various species [10, 19, 21, 22], and it also finds numerous applications for substrates that can become inhibitory, such as phenol, ethanol, or volatile fatty acids [12, 23–25]. In another class of applications, inhibitory effects on photosynthesis have been observed after exposure to strong light intensities, causing specific damage occurs to photosynthetic units, as discussed by B. Kok in [26]:

If algae are exposed to very strong light, the maximum photosynthetic rate
does not persist; sooner or later it decreases and may ultimately drop to
zero.

To account for this phenomenon of photoinhibition, the Haldane model has been used to describe the effect of excess light on photosynthetic microorganisms, and its effectiveness has also been validated experimentally [11, 27–30].

Despite the widespread use of the Haldane model to represent inhibitory effects, its practical application often proves intricate due to the variety of parameterizations proposed in the literature [10, 11, 19, 27]. Mathematically, this model can be expressed as the ratio of a term proportional to the substrate concentration (or the light intensity) and a second-order polynomial. In other words, the inverse of the yield (ratio of the factor to the growth rate) is a quadratic polynomial. Although numerous parameterizations of the Haldane model have been proposed, it can be shown that they are actually mathematically equivalent. This then raises three main questions.

- Q1. Which parameterizations are preferable in terms of parameter identifiability process and resulting model accuracy ?
- Q2. Are there alternative equivalent parameterizations that are easier to estimate and can provide higher accuracy ?

60
61
Q3. How can different parameterizations of a same model be calibrated and
systematically compared ?

62
63
To the best of our knowledge, no systematic study has yet addressed these questions.
Therefore, we aim to provide such an analysis in this paper.

64
65
The current study is organized as follows. We first review existing parameterizations
in the literatures and show their mathematical equivalence. Meanwhile, we present a
66
new equivalent parameterization requiring fewer parameters. We then restrict to a
single inhibitory effect in order to investigate the identification and calibration
67
properties of these parameterizations. The sources of experimental data and the
methods used in our analyses are then described. To select the best parameterization,
68
we compare results obtained using standard model selection criteria with those derived
from a new enhanced criterion. Finally, we present some numerical experiments and
70
conclude with a detailed discussion with some comments on the findings of our studies.
71
72

73 Mathematical analysis

74
75
Generally speaking, parameterizations of the Haldane are not always presented
consistently in the literature, and the use of different parameterizations can sometimes
be misleading. To address this, we briefly provide a historical review of the four major
76
parameterizations of the Haldane model to describe microbial growth kinetics, and then
analyze mathematically their relationship.
77
78

79 Historical review

80
81
The original model was introduced by J.B.S. Haldane in 1930 in the context of enzymes
kinetics [20], and it was first adapted by J.F. Andrews in 1968 for microbial growth
under substrate inhibition in [19]. Thus, the model is often referred to as the
82
Haldane–Andrews model in the context of microbial growth kinetics. This model uses
three parameters to describe the growth kinetics:
83
84

$$85 \quad \mu^1(x) = \frac{\hat{\mu}}{1 + \frac{K_x}{x} + \frac{x}{K_i}}, \quad (1)$$

86
87
where $\hat{\mu}$ is the maximum specific growth rate in the absence of inhibition (inverse of
time), K_x is the saturation constant, numerically equals lowest concentration of
substrate at which the specific growth rate is equal to one-half the maximum specific
88
growth rate in the absence of inhibition (mass over volume), and K_i is the inhibition
89
constant, numerically equals the highest substrate concentration at which the specific
90
growth rate is equal to one-half the maximum specific growth rate in the absence of
91
inhibition (mass over volume). This parameterization has been well studied and
calibrated with experimental data of various species and different substrate inhibitors,
e.g., see [21, 31, 32].
92
93

94
95
In subsequent work, V.H. Edwards in 1970 used a similar notation for another triplet
(μ_m, K_x, K_i) in [10] to describe microbial growth kinetics:

$$96 \quad \mu^2(x) = \frac{\mu_m x}{(x + K_x)(1 + \frac{x}{K_i})}, \quad (2)$$

97
98
where the interpretation of each parameter was not explicitly specified. Edwards further
claimed in [10] that this equation was also derived by Haldane. However, the two
99
equations (1) and (2) are actually not the same. Dividing both numerator and
denominator of (2) by x yields

$$99 \quad \mu^2(x) = \frac{\mu_m}{(1 + \frac{K_x}{x})(1 + \frac{x}{K_i})} = \frac{\mu_m}{1 + \frac{K_x}{x} + \frac{x}{K_i} + \frac{K_x}{K_i}},$$

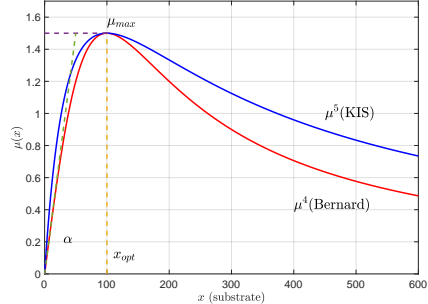


Fig 1. Representation of two Haldane parameterizations. Red curve: parameterization of Bernard–Rémond (4) with the three fundamental parameters, μ_{\max} the maximum growth rate for the optimal irradiance x_{opt} , and α the initial slope. Blue curve: new parameterization KIS (5) with only two parameters γ_{\max} and x^* .

which is different from (1). Therefore, despite the same notation K_x and K_i in both parameterizations, their interpretations may not coincide. This ambiguity leads to potential identifiability issue, which will be further discussed in the following. Nevertheless, the use of Edwards-type parameterization can be traced back in 1962 by B. Boon and H. Laudelout [33], who applied it to describe the kinetics of Nitrite oxidation by *Nitrobacter*.

In 1978, J.C.H. Peeters and P.H.C. Eilers proposed in [27] a different parameterization of the Haldane model to describe the photoinhibition effect of microorganisms. They rather use three arbitrary parameters a , b , and c to represent the growth kinetics:

$$\mu^3(x) = \frac{x}{ax^2 + bx + c}. \quad (3)$$

In particular, they noted in [27] that

The parameters values do not follow from the theory; they have to be fitted for real measurements.

Although the authors did not mention explicitly the Haldane model in [27], their work marks the first attempt to apply this model to describe the relationship between light intensity and photosynthesis, and it has been widely used and calibrated by experimental data, e.g., see [28, 30].

More than three decades later, O. Bernard and B. Rémond proposed in 2012 a new parameterization of the Haldane model in [11] to account for the influence of light on phytoplankton growth rate. This parameterization also contains three parameters given by

$$\mu^4(x) = \frac{\mu_{\max}x}{x + \frac{\mu_{\max}}{\alpha}(\frac{x}{x_{\text{opt}}} - 1)^2}, \quad (4)$$

where μ_{\max} is the maximum growth rate for the optimal irradiance (s^{-1}), α is the initial slope of the light response curve ($\mu\text{mol}^{-1} \text{photons m}^2$), and x_{opt} is the value of the irradiance for which the growth is maximal ($\mu\text{mol photons m}^{-2} \text{s}^{-1}$). One major advantage of this parameterization is the physical meaning of each parameter. Indeed, the growth kinetics for this parameterization is depicted in Fig. 1 (red curve) together with three parameters (μ_{\max} , x_{opt} , α). We observe that these three parameters are mathematically fundamental to characterize the growth curve. This also allows a better performance in the calibration process, as shown later in our numerical experiments.

Equivalent relationship between parameterizations

As the three parameters $(\mu_{\max}, \alpha, x_{\text{opt}})$ in the parameterization of Bernard–Rémond (4) have a clear physical meaning, and parameters in the other parameterizations do not have a direct interpretation. We use (4) as our reference and $(\mu_{\max}, \alpha, x_{\text{opt}})$ as our fundamental parameters. To show that four equations (1)-(4) are all mathematically equivalent, we rewrite each parameterization in the same form as our reference, and we find,

- parameterization of Andrews (1):

$$\hat{\mu} = \frac{\mu_{\max}\alpha x_{\text{opt}}}{\alpha x_{\text{opt}} - 2\mu_{\max}}, \quad K_x = \frac{\mu_{\max}x_{\text{opt}}}{\alpha x_{\text{opt}} - 2\mu_{\max}}, \quad K_i = \frac{x_{\text{opt}}(x_{\text{opt}}\alpha - 2\mu_{\max})}{\mu_{\max}},$$

with the units of each parameter $\hat{\mu}$ (inverse of time), K_x and K_i (same as x). Note that the parameters of this model are complex combinations of the three fundamental parameters.

- parameterization of Edwards (2):

$$\mu_m = \alpha K_x, \quad K_x K_i = x_{\text{opt}}^2, \quad K_x + K_i = \frac{(\alpha x_{\text{opt}} - 2\mu_{\max})x_{\text{opt}}}{\mu_{\max}},$$

with the unit of μ_m (inverse of time), K_x and K_i the same units as x . Note that there are two (equivalent) possible values for the couple (K_x, K_i) , which illustrates the dramatic identifiability issue of this model in practice, e.g., see [34, Tip 6].

- parameterization of Peeters–Eilers (3):

$$a = \frac{1}{\alpha x_{\text{opt}}^2}, \quad b = \frac{1}{\mu_{\max}} - \frac{2}{\alpha x_{\text{opt}}}, \quad c = \frac{1}{\alpha},$$

with units for b (time), a (time per unit of x) and c (time times unit of x). We observe that the parameter c is directly connected to α , and the parameter a is deduced from α and x_{opt} . The parameter b results from the three fundamental parameters.

This not only shows the equivalent relationship of these four major parameterizations, but also reveals the link between each parameter.

New parameterization: KIS

Each of the four parameterizations (1)-(4) contains three parameters to describe microbial growth kinetics, and one of the main proposes of our work (Q2) is also to seek alternative parameterizations with fewer parameters. For this reason, we introduce a new Haldane type parameterization with only two parameters to characterize the growth:

$$\mu^5(x) = 4\gamma_{\max} \frac{xx^*}{(x + x^*)^2}. \quad (5)$$

Before discussing the physical interpretation of the two parameters γ_{\max} and x^* , we first show the equivalence between (5) and existing parameterizations. Once again, we rewrite (5) in the form of (4) and obtain directly

$$\gamma_{\max} = \mu_{\max}, \quad x^* = x_{\text{opt}}, \quad \frac{4\gamma_{\max}}{x^*} = \alpha.$$

Mathematically speaking, the parameters (γ_{\max}, x^*) are exactly the same to $(\mu_{\max}, x_{\text{opt}})$ as long as they satisfy $4\gamma_{\max}/x^* = \alpha$. Furthermore, the parameter x^* (same unit as x) corresponds to the value of x for which the growth rate is the maximum, and the parameter γ_{\max} (inverse of time) is the maximum growth rate obtained for x^* . The resulting growth curve is also illustrated in Fig. 1 (blue curve). Although (γ_{\max}, x^*) and $(\mu_{\max}, x_{\text{opt}})$ seem very similar in Fig. 1, their values are chosen differently such that $4\frac{\gamma_{\max}}{x^*} \neq \alpha$, which helps to distinguish the two curves. We observe that this new parameterization of the Haldane model with only two parameters can also well represent the growth kinetics with inhibition effect. Each parameter has a clear physical interpretation, which is advantageous for calibration process and sensitivity analysis, and will be further discussed in our numerical experiments. From a modelling perspective, a model with fewer parameters that still captures the essential features of the phenomenon is generally preferable. The proposed two-parameter formulation (5) follows exactly this principle and provides a new idea of modelling inhibitory effect: *Keep It Simple (KIS)*.

Materials and methods

All five parameterizations (1)-(5) are mathematically equivalent one to the other, the only difference is from the calibration and identification viewpoint. To study the identifiability and eventually select the best parameterization (Q1), we focus on the specific inhibition example of microalgae kinetics growth with respect to the irradiance. From now on, the variable x in (1)-(5) represents the irradiance with the unit ($\mu\text{mol photons m}^{-2} \text{s}^{-1}$). We assess the uncertainty associated with the parameterization predictions and identify the most appropriate parameter values of each parameterization for the given experimental conditions.

Experimental data

The experimental data are taken from the literature [35, 36] that contains in total eight different microalgae species. For self-completeness, we briefly describe these experiments.

Growth response with *Skeletonema costatum*

Anning et al. [35] study the growth of the diatom *Skeletonema costatum* strain CCMP 1332 (Plymouth Culture Collection). The algae cells are cultured under the same conditions, except for the irradiance levels. Here, we focus on the curve obtained for the pre-acclimation at $1200 \mu\text{mol photons m}^{-2} \text{s}^{-1}$, for which the photoinhibition is more marked. Labelled $\text{NaH}^{14}\text{CO}_3$ was used to culture algal cells simultaneously over a gradient of irradiance to determine photosynthetic carbon fixation.

Growth response via oxymetry for seven species of phytoplankton

Yang et al. [36] investigate the photosynthetic response of seven strains of phytoplankton, comprising three strains of marine phytoplankton (*Isochrysis galbana*, *Dunaliella salina*, and *Platymonas subcordiformis*) and four strains of freshwater phytoplankton (*Chlorococcum sp.* FACHB-1556, *Microcystis aeruginosa* FACHB-905, *Microcystis wesenbergii* FACHB-1112, and *Scenedesmus obliquus* FACHB-116.). Cells are cultured at an irradiance of $60 \mu\text{mol photons m}^{-2} \text{s}^{-1}$ for 12 hours per day and at a temperature of $26 \pm 1^\circ\text{C}$ for 7 to 10 days. The cells are then subjected to increasing levels of irradiance, ranging from 0 to $1200 (\mu\text{mol photons m}^{-2} \text{s}^{-1})$, provided by a

digital LED light source at a temperature of $25 \pm 1^\circ\text{C}$. The oxygen-evolving rate is
204 measured by using dissolved oxygen measurements.
205

Parameter identification

To identify appropriate parameterizations from the experimental data, we need to
206 introduce some notations. Let us denote by θ^k the parameter set corresponding to the
207 parameterization μ^k :
208

$$\theta^1 = (\hat{\mu}, K_x, K_i) \text{ for } \mu^1 \text{ in (1), } \theta^2 = (\mu_m, K_x, K_i) \text{ for } \mu^2 \text{ in (2), } \theta^3 = (a, b, c) \text{ for } \mu^3 \text{ in (3),} \\ 209 \theta^4 = (\mu_{\max}, \alpha, x_{\text{opt}}) \text{ for } \mu^4 \text{ in (4), } \theta^5 = (\gamma_{\max}, x^*) \text{ for } \mu^5 \text{ in (5).}$$

We denote by m the number of parameters and by θ_j^k ($j = 1, \dots, m$) each element of
210 the parameter set θ^k . For instance, $\theta_1^4 = \mu_{\max}$, $\theta_2^4 = \alpha$, and $\theta_3^4 = x_{\text{opt}}$ in the
211 parameterization of Bernard–Rémond (4). Note that $m = 3$ for
212 parameterizations (1)-(4), and $m = 2$ for the parameterization (5). For each microalgae
213 species, we denote by $(x_i)_{i=1}^n$ the irradiance samples (with n the size of the samples)
214 and $\mu_{\exp}(x_i)$ the associated experimental estimations of the growth rate. We denote by
215 $\mu^k(x_i, \theta^k)$ the growth rate evaluated in the light sample x_i using the parameterization
216 μ^k . The sum of the squared error (SSE) [37, 38] is given by:
217

$$\text{SSE} := \sum_{i=1}^n (\mu_{\exp}(x_i) - \mu^k(x_i, \theta^k))^2. \quad (6)$$

With this, for each parameterization μ^k , the parameter identification problem can be
218 stated as a standard nonlinear least-squares optimization problem:
219

$$\begin{aligned} \min_{\theta^k} \quad & \text{SSE} = \sum_{i=1}^n (\mu_{\exp}(x_i) - \mu^k(x_i, \theta^k))^2, \\ \text{subject to} \quad & \theta_{\min}^k \leq \theta^k \leq \theta_{\max}^k, \end{aligned} \quad (7)$$

where $[\theta_{\min}^k, \theta_{\max}^k]$ is an appropriate theoretical range of the parameter values. A
220 parameter set θ^k that solves this optimization problem is a local optimal parameter set.
221 Since the uniqueness of the optimum is not guaranteed, we choose the best parameter
222 set as the local optimum for which the SSE value is the smallest. Numerically, we use
223 the Nelder–Mead simplex algorithm [39] implemented in the *fminsearch* function of
224 Matlab.
225

Sensitivity analysis

Once the best parameter set θ^k has been identified, we compute the sensitivity
226 equations to determine the Fisher information matrix (FIM) to compare different
227 parameterizations [40]. The FIM is defined by,
228

$$F := \left(\frac{\partial \mu^k}{\partial \theta^k}(x) \right)^T Q \frac{\partial \mu^k}{\partial \theta^k}(x), \quad (8)$$

where Q is a square matrix representing the inverse of the covariance matrix of the
229 measurement error. This information was not provided for $\mu_{\exp}(x_i)$ in the considered
230 experimental data. We therefore assumed a 10% standard variation for each
231 measurement, except for the lowest values where this value is saturated at a minimum
232 level, following the strategy of [41]. More formally, we assume that the standard
233 variation vector is:
234

$$W := \max_{i=1, \dots, n} \left(0.1 \mu_{\exp}(x_i), 0.02 \max_{i=1, \dots, n} (\mu_{\exp}(x_i)) \right). \quad (9)$$

We then define Q as a diagonal matrix with the entries $Q_{ii} := 1/W_i^2$.
236

For each parameter set θ^k , the standard deviation is defined by
237

$$\sigma := s\sqrt{n\text{diag}(V)}, \quad (10)$$

where $V := F^{-1}$ is the covariance matrix of parameter estimation error, and s is the residual mean square with:
238
239

$$s^2 := \frac{\sum_{i=1}^n (\mu^k(x_i, \theta^k) - \mu_{\text{exp}}(x_i))^T Q_i (\mu(x_i, \theta^k) - \mu_{\text{exp}}(x_i))}{n - m}. \quad (11)$$

From the parameter standard deviation, we can compute the prediction interval (PI)
240 by
241

$$PI := \mu^k \pm Ze, \quad (12)$$

where Z is the value of Student's t -distribution choosing a significance level 0.05, and e
242 is the error propagation with $e := \sqrt{\sum_{j=1}^m (\frac{\partial \mu^k}{\partial \theta_j^k})^2 \sigma_j^2}$. The adequacy of the
243 parameterization μ^k with the experimental measurements is the first criterion to assess
244 its performance.
245

Additionally, the sensitivity of the parameter θ_j^k is computed as the normalized
246 sensitivity [42]
247

$$S_j := \left(\frac{\sigma_j}{e} \frac{\partial \mu^k}{\partial \theta_j^k} \right)^2. \quad (13)$$

Parameterization selection criteria: PEMAC

The most popular model selection criteria are Akaike's information criterion
249 (AIC) [37, 43, 44] and Bayesian information criterion (BIC) [45, 46]. They are used in the
250 analysis of empirical data that account for the differences in the model degrees of
251 freedom. By comparing the AIC and BIC values and the identification results, we can
252 determine the best model. We recall here the definition of AIC
253

$$AIC := n \log\left(\frac{SSE}{n}\right) + 2(m + 1). \quad (14)$$

For small-samples, when $\frac{n}{m+1} < 40$, the AIC becomes the corrected Akaike information
254 criterion (AIC_c), given by :
255

$$AIC_c := AIC + \frac{2(m + 1)(m + 2)}{n - m - 2}. \quad (15)$$

The Bayesian information criterion is given by:
256

$$BIC := n \log\left(\frac{SSE}{n}\right) + (m + 1) \log(n). \quad (16)$$

Both criteria have been proven to be very effective when comparing and selecting
257 different models. However, they become less efficient when it comes to distinguishing
258 equivalent parameterizations of the same model. To address this issue (Q3), we
259 introduce a new criterion based on the criteria AIC_c and BIC to improve the sensitivity
260 to evaluate various parameterizations of one model. Let us denote by \bar{e} the average of
261 the error propagation e , which is an important criterion for qualifying the model
262 accuracy
263

$$\bar{e} := \frac{1}{n} \sum_{i=1}^n \sqrt{\sum_{j=1}^m \left(\frac{\partial \mu^k}{\partial \theta_j^k}(x_i) \right)^2 \sigma_j^2}. \quad (17)$$

		1	2	3	4	5	6	7	8
(1)	$\hat{\mu}$	3.1756×10^{-4}	0.9330	0.1050	0.0518	0.0458	-1.9147	11.9335	1.5156
	K_x	3504.5484	9240.9056	398.3028	69.4167	138.2674	-3875.0132	30429.2456	4324.3801
	K_i	265.8140	52.6380	484.0769	922.3136	848.7246	-29.7342	3.3641	54.3864
SSE		1.1164×10^{-10}	1.2346×10^{-5}	1.0841×10^{-5}	4.6218×10^{-5}	1.0985×10^{-5}	6.0475×10^{-5}	3.5333×10^{-5}	3.1000×10^{-5}
(2)	μ_m	1.5234×10^{-4}	0.1318	0.1449	0.0565	0.0576	0.3138	0.2241	0.2989
	K_x	1273.9800	914.5639	458.7265	75.6161	173.8978	343.2328	323.1022	544.4024
	K_i	1274.3248	914.5640	458.7265	846.6974	674.8267	343.2328	323.1022	544.4024
SSE		1.5685×10^{-10}	4.3482×10^{-5}	2.0970×10^{-5}	4.6218×10^{-5}	1.0985×10^{-5}	6.0296×10^{-4}	2.8402×10^{-4}	3.0619×10^{-4}
(3)	a	11.8466	0.0204	0.0197	0.0209	0.0257	0.0176	0.0249	0.0121
	b	3148.9876	1.0718	9.5276	19.2887	21.8174	-0.5223	0.0838	0.6598
	c	1.1036×10^7	9904.8464	3794.8752	1338.9598	3016.6396	2023.8331	2549.9064	2853.2691
SSE		1.1164×10^{-10}	1.2346×10^{-5}	1.0841×10^{-5}	4.6218×10^{-5}	1.0985×10^{-5}	6.0475×10^{-5}	3.5333×10^{-5}	3.1000×10^{-5}
(4)	μ_{\max}	3.8436×10^{-5}	0.0339	0.0373	0.0335	0.0254	0.0877	0.0624	0.0805
	α	9.0614×10^{-8}	1.0096×10^{-4}	2.6351×10^{-4}	7.4685×10^{-4}	3.3149×10^{-4}	4.9411×10^{-4}	3.9217×10^{-4}	3.5048×10^{-4}
	x_{opt}	965.1726	697.4415	439.1005	253.0296	342.5652	339.4417	319.9471	484.9611
SSE		1.1164×10^{-10}	1.2346×10^{-5}	1.0841×10^{-5}	4.6218×10^{-5}	1.0985×10^{-5}	6.0475×10^{-5}	3.5333×10^{-5}	3.1000×10^{-5}
(5)	γ_{\max}	3.8086×10^{-5}	0.0329	0.0362	0.0351	0.0257	0.0784	0.0560	0.0747
	x^*	1273.9800	914.5640	458.7265	248.7247	338.0766	343.2328	323.1022	544.4024
SSE		1.5685×10^{-10}	4.3482×10^{-5}	2.0970×10^{-5}	6.8655×10^{-5}	1.2139×10^{-5}	6.0296×10^{-4}	2.8402×10^{-4}	3.0619×10^{-4}

Table 1. Best estimates of five parameterizations (1)-(5) for each microalgae species. (1. *Skeletonema costatum*, 2. *Isochrysis galbana*, 3. *Dunaliella salina*, 4. *Platymonas subcordiformis*, 5. *Chlorococcum sp.* FACHB-1556, 6. *Microcystis aeruginosa* FACHB-905, 7. *Microcystis wesenbergii* FACHB-1112, 8. *Scenedesmus obliquus* FACHB-116).

The new criterion, namely the Propagated Error Modified Akaike Criterion (PEMAC), is defined by

$$\text{PEMAC} := \begin{cases} 2n \log(\bar{e}) + n \log\left(\frac{\text{SSE}}{n}\right) \\ \quad + (m+1) \log n, & \frac{n}{m+1} \geq 40, \\ 2n \log(\bar{e}) + n \log\left(\frac{\text{SSE}}{n}\right) \\ \quad + \frac{2(m+1)(m+2)}{n-m-2}, & \frac{n}{m+1} < 40. \end{cases}$$

We will compare our criterion with AIC_c and BIC, and show that our criterion provides better performance in terms of selecting the best parameterizations of the same model.

Results

We now compare numerical performance of the four existing parameterizations (1)-(4) and our new parameterization (5). Our analyses are based on the experimental data for the light response of eight different microalgae species. For each species, we identify the most appropriate parameter values, present the sensitivity and the identifiability of each parameterization.

Parameter identification results

For each parameterization μ^k among (1)-(5), the optimal parameter set θ^k varies under different experimental conditions and different microalgae species. Table 1 presents the optimal parameter sets and the SSE values for each parameterization and for eight microalgae species. The SSE values for the species *Skeletonema costatum* is smaller not only due to the quality of the fit, but also because the measurement method is different, and with different units. This also reflects on the identified parameter values, e.g., the value obtained for μ_{\max} is 3.8436×10^{-5} with the unit s⁻¹, but h⁻¹ for the rest.

	1			2			3			4			5			6			7			8		
(1)	$\hat{\mu}$	K_x	K_i																					
$\hat{\mu}$	1.00	1.00	-1.00	1.00	1.00	-1.00	1.00	0.99	-0.99	1.00	0.93	-0.95	1.00	0.96	-0.96	1.00	1.00	-1.00	1.00	1.00	-1.00	1.00	1.00	-1.00
K_x	1.00	1.00	-1.00	1.00	1.00	-1.00	0.99	1.00	-0.97	0.93	1.00	-0.86	0.96	1.00	-0.91	1.00	1.00	-1.00	1.00	1.00	-1.00	1.00	1.00	-1.00
K_i	-1.00	-1.00	1.00	-1.00	-1.00	1.00	-0.99	-0.97	1.00	-0.95	-0.86	1.00	-0.96	-0.91	1.00	-1.00	-1.00	1.00	-1.00	1.00	-1.00	-1.00	1.00	-1.00
(2)	μ_m	K_x	K_i																					
μ_m	-	-	-	-	-	-	-	-	-	1.00	0.96	-0.97	1.00	0.99	-0.99	-	-	-	-	-	-	-	-	-
K_x	-	-	-	-	-	-	-	-	-	0.96	1.00	-0.91	0.99	1.00	-0.97	-	-	-	-	-	-	-	-	-
K_i	-	-	-	-	-	-	-	-	-	-0.97	0.91	1.00	-0.99	-0.97	1.00	-	-	-	-	-	-	-	-	-
(3)	a	b	c																					
a	1.00	-0.95	0.72	1.00	-0.94	0.72	1.00	-0.90	0.62	1.00	-0.87	0.55	1.00	-0.89	0.58	1.00	-0.91	0.69	1.00	-0.90	0.64	1.00	-0.92	0.70
b	-0.95	1.00	-0.85	-0.94	1.00	-0.86	-0.90	1.00	-0.79	-0.87	1.00	-0.72	-0.89	1.00	-0.74	-0.91	1.00	-0.86	-0.90	1.00	-0.83	-0.92	1.00	-0.85
c	0.72	-0.85	1.00	0.72	-0.86	1.00	0.62	-0.79	1.00	0.55	-0.72	1.00	0.58	-0.74	1.00	0.69	-0.86	1.00	0.64	-0.83	1.00	0.70	-0.85	1.00
(4)	μ_{\max}	α	x_{opt}																					
μ_{\max}	1.00	-0.30	0.05	1.00	-0.39	-0.07	1.00	-0.47	-0.32	1.00	-0.46	-0.38	1.00	-0.47	-0.39	1.00	-0.50	-0.19	1.00	-0.46	-0.24	1.00	-0.51	-0.30
α	-0.30	1.00	0.53	-0.39	1.00	0.47	-0.47	1.00	0.18	-0.46	1.00	-0.09	-0.47	1.00	0.11	-0.50	1.00	-0.27	-0.46	1.00	-0.23	-0.51	1.00	0.18
x_{opt}	0.05	0.53	1.00	-0.07	0.47	1.00	-0.32	0.18	1.00	-0.38	-0.09	1.00	-0.39	0.11	1.00	-0.19	-0.27	1.00	-0.24	-0.23	1.00	-0.30	0.18	1.00
(5)	γ_{\max}	x^*	-																					
γ_{\max}	1.00	-0.81	-	1.00	-0.78	-	1.00	-0.39	-	1.00	0.07	-	1.00	-0.18	-	1.00	-0.05	1.00	-0.14	1.00	-0.48	1.00	-0.48	-
x^*	-0.81	1.00	-	-0.78	1.00	-	-0.39	1.00	-	0.07	1.00	-	-0.18	1.00	-	-0.05	1.00	-	-0.14	1.00	-	-0.48	1.00	-

Table 2. Correlation matrix of parameter estimation error of five parameterizations (1)-(5) for eight microalgae species (1. *Skeletonema costatum*, 2. *Isochrysis galbana*, 3. *Dunaliella salina*, 4. *Platymonas subcordiformis*, 5. *Chlorococcum sp.* FACHB-1556, 6. *Microcystis aeruginosa* FACHB-905, 7. *Microcystis wesenbergii* FACHB-1112, 8. *Scenedesmus obliquus* FACHB-116). Note that “–” represents the case where the Fisher information matrix F is singular, and we cannot obtain an accurate result.

Regarding the seven other species, the SSE values are on the scale of 10^{-5} , except for the parameterizations of Edwards (2) and KIS (5) with the species *Microcystis wesenbergii* FACHB-1112, *Scenedesmus obliquus* FACHB-116 and *Chlorococcum sp.* FACHB-1556, where the SSE values are on the scale of 10^{-4} . This reveals that the parameterizations of Andrews (1), Peeters–Eilers (3), and Bernard–Rémond (4) in their identified parameter sets fit slightly better the experimental data in [36] compared to Edwards (2) and KIS (5). Although the parameterization of Bernard–Rémond (4) is specifically designed to study the influence of irradiance on phytoplankton growth rate, we observe that there are no great differences in its SSE values with the other four parameterizations. This is not surprising since the underlying mathematical model is identical, and only the way the parameters are expressed is changing. Moreover, we observe that, in general, the identified values of γ_{\max} and x^* in KIS (5) are quite similar to μ_{\max} and x_{opt} in Bernard–Rémond (4). This further confirms the physical meaning of the two parameters in the proposed new parameterization (5). For the following numerical tests, we will use the optimal parameter values given in Table 1.

Correlation matrix of parameter estimation error

Based on the covariance matrix of the parameter estimation error V , we compute the correlation matrix of the parameter estimation error, and illustrate in Table 2 for all five parameterizations and eight microalgae species. We consider that two parameters θ_i^k and θ_j^k are correlated if the absolute value of their correlation exceeds 0.9. Taking this into account, we observe that the three fundamental parameters ($\mu_{\max}, \alpha, x_{\text{opt}}$) in the parameterization of Bernard–Rémond (4) are rather uncorrelated with each other, and same observation goes for the two parameters (γ_{\max}, x^*) in the parameterization KIS (5). On the other hand, the three parameters ($\hat{\mu}, K_x, K_i$) in the parameterization of Andrews (1) are strongly correlated. This is expected since all three parameters are complex combination of the three fundamental parameters, as shown in the previous section. There are only two microalgae species for which we are able to determine the correlation matrix for the parameterization of Edwards (2). This is due to the fact that the related Fisher information matrix F is singular. For these two species, we observe once again a strong correlation between the three parameters (μ_m, K_x, K_i) in (2). This further confirms the identifiability issue reported in [34]. Regarding the

parameterization of Peeters–Eilers (3), there is a strong correlation between the parameters a and b , and both are rather uncorrelated with the parameter c . The correlation coefficient between the parameters assesses whether the parameters are independent. If one of the parameters is not independent, then the correlated parameters are likely to produce similar information, and the parameterization is thus less efficient. Based on our observations, parameterizations of Bernard–Rémond (4) as well as KIS (5) are more suitable to represent the growth rate with respect to irradiance for the eight microalgae species.

Best parameterization of the inhibition kinetics

In general, the minimum value of AIC_c or BIC reveals the best trade-off between the number of parameters m and the ability to fit the data among different models. However, this becomes less clear for selecting equivalent parameterizations of one model. Table 3 presents the AIC_c , BIC values as well as the values obtained using the new criterion PEMAC for the five parameterizations (1)–(5) and for eight microalgae species. We observe that the AIC_c and BIC values do not vary significantly among the five

	(1)	(2)	(3)	(4)	(5)
<i>Skeletonema costatum</i>					
AIC_c	-561.7971	-554.3161	-561.7971	-561.7971	-557.3357
BIC	-559.7858	-552.3049	-559.7858	-559.7858	-555.3959
PEMAC	-928.9370	-	-1028.5730	-1082.4752	-1060.1172
<i>Isochrysis galbana</i>					
AIC_c	-167.2731	-150.9055	-167.2731	-167.2731	-155.2388
BIC	-170.0133	-153.6457	-170.0133	-170.0133	-156.2106
PEMAC	-211.7551	-	-302.2497	-333.9981	-296.7996
<i>Dunaliella salina</i>					
AIC_c	-168.9626	-160.3860	-168.9626	-168.9626	-164.7193
BIC	-171.7028	-163.1262	-171.7028	-171.7028	-165.6911
PEMAC	-287.4636	-	-317.7917	-341.5794	-329.9519
<i>Platymonas subcordiformis</i>					
AIC_c	-150.1121	-150.1121	-150.1121	-150.1121	-149.3011
BIC	-152.8523	-152.8523	-152.8523	-152.8523	-150.2729
PEMAC	-260.5042	-252.3863	-275.0006	-290.3377	-299.8248
<i>Chlorococcum sp.</i> FACHB-1556					
AIC_c	-168.7907	-168.7907	-168.7907	-168.7907	-171.8261
BIC	-171.5309	-171.5309	-171.5309	-171.5309	-172.7979
PEMAC	-295.6872	-275.4283	-314.1104	-333.2404	-348.9473
<i>Microcystis aeruginosa</i> FACHB-1556					
AIC_c	-132.6640	-105.0685	-132.6640	-132.6640	-109.7828
BIC	-136.4387	-108.8432	-136.4387	-136.4387	-111.3281
PEMAC	-157.6629	-	-236.6074	-259.9892	-219.0630
<i>Microcystis wesenbergii</i> FACHB-1112					
AIC_c	-153.6035	-126.5084	-153.6035	-153.6035	-130.8417
BIC	-156.3437	-129.2486	-156.3437	-156.3437	-131.8136
PEMAC	-137.3329	-	-279.3771	-302.4023	-262.9083
<i>Scenedesmus obliquus</i> FACHB-116					
AIC_c	-140.6828	-113.2002	-140.6828	-140.6828	-117.9145
BIC	-144.4574	-116.9749	-144.4574	-144.4574	-119.4598
PEMAC	-177.7300	-	-252.0564	-278.5561	-232.4748

Table 3. The AIC_c , BIC and PEMAC values of the parameterizations (1)–(5) for each microalgae species in [35] and [36].

parameterizations, especially for the species *Platymonas subcordiformis* and *Chlorococcum sp.* FACHB-1556. Thus, based on the values of AIC_c and BIC , it is less clear which parameterization is better among (1)–(5). This ambiguity disappears when using our new criterion PEMAC. Indeed, there is a clear difference in the PEMAC value between the five parameterizations, even in the case of the species *Platymonas subcordiformis* and *Chlorococcum sp.* FACHB-1556, where the criteria AIC_c and BIC are unable to distinguish. Furthermore, this new criterion PEMAC also takes into account the identifiability issue of the parameterization of Edwards (2), which are

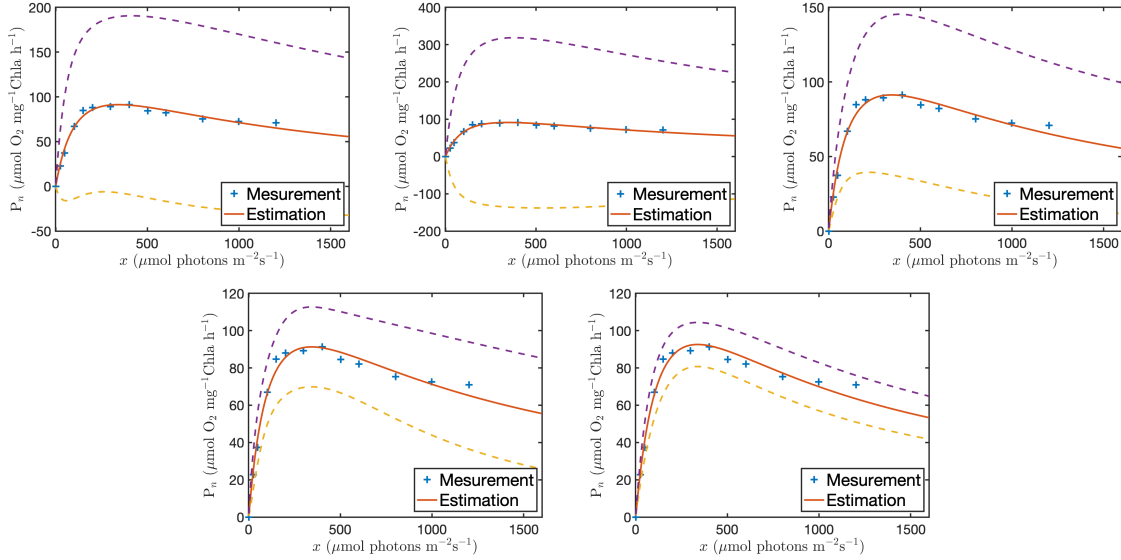


Fig 2. Prediction intervals of five parameterizations with respect to the irradiance for the experimental data of *Chlorococcum sp.* FACHB-1556 in [36]. In each figure, the blue points are the experimental data, the red curve is the one obtained using the parameter values computed in Table 1, the yellow and purple curves represent the prediction interval. Top left: Andrew (1). Top middle: Edwards (2). Top right: Peeters–Eilers (3). Bottom left: Bernard–Rémond (4). Bottom right: KIS (5).

ignored by the criteria AIC_c and BIC, as we need the Fisher information matrix F to compute the average error propagation value (17) in PEMAC. Therefore, we can observe again the identifiability problem of Edwards using PEMAC. In terms of the performance, we observe that the parameterization of Bernard–Rémond (4) has the minimum value of PEMAC most of the time, except for the species *Platymonus subcordiformis* and *Chlorococcum sp.* FACHB-1556, where the parameterization KIS (5) has the minimum PEMAC value. In general, our new parameterization KIS shows competitive results with that of Bernard–Rémond (4), meaning that KIS also provides a good representation of the growth rate with respect to the irradiance using only two parameters.

Prediction interval

To further check the quality of using each parameterization to characterize the growth rate, Fig. 2 illustrates the prediction interval (12) of each parameterization for *Chlorococcum sp.* FACHB-1556 as an example. From the scale and shape of the prediction intervals, we observe that both parameterizations of Bernard–Rémond (4) and KIS (5) provide a relatively good prediction compared with the other three parameterizations (1)-(3). Between these two, the prediction interval of KIS is even more fine than that of Bernard–Rémond, showing that our new parameterization can provide more accurate prediction in this example. On the other hand, the parameterization of Edwards (2) provides the worst prediction interval, revealing also the accuracy issue of this parameterization. In general, we observe similar behavior of these five parameterizations for the other seven species, and their prediction interval curves are presented in Fig. A.1 - A.8 in S1 Appendix for the sake of compactness. In terms of performance, both parameterizations of Bernard–Rémond (4) and KIS (5) always provide good prediction for all eight microalgae species. Note also that due to the singularity issue of the Fisher information matrix F obtained for the

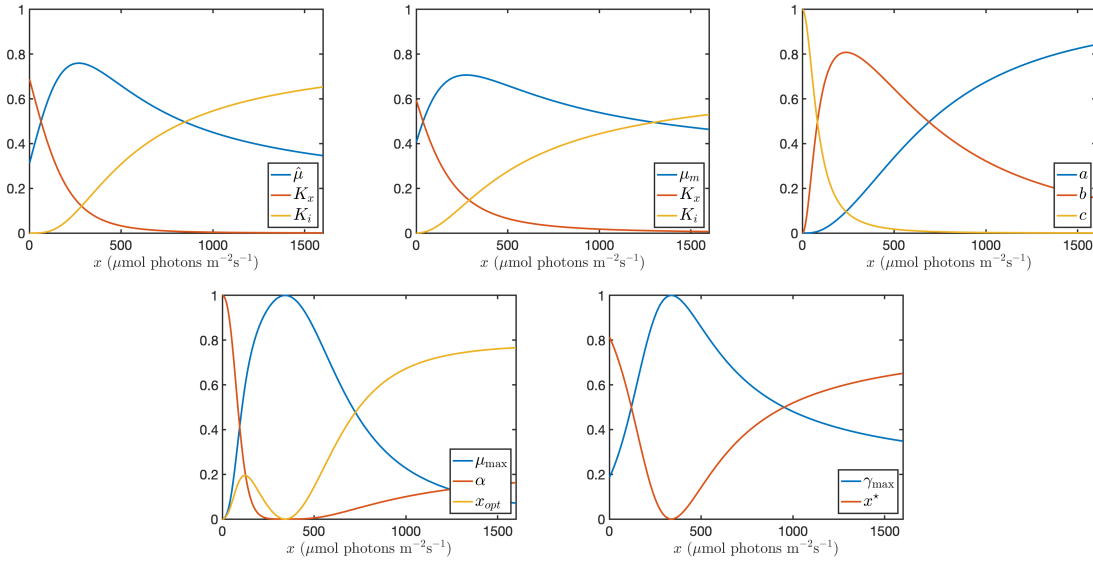


Fig 3. Normalized sensitivity computed using (13) for each parameter of five parameterizations with respect to the irradiance x for the experimental data of *Chlorococcum sp.* FACHB-1556 [36]. Top left: Andrew (1). Top middle: Edwards (2). Top right: Peeters–Eilers (3). Bottom left: Bernard–Rémond (4). Bottom right: KIS (5).

parameterization of Edwards (2), we are only able to show the prediction interval of Edwards for two species *Platymonas subcordiformis* and *Chlorococcum sp.* FACHB-1556.

Parameter sensitivity

We also study the parameter sensitivity using the normalized sensitivity (13). Fig. 3 presents the normalized sensitivity of each parameterization μ^k with respect to the related parameter set θ^k for *Chlorococcum sp.* FACHB-1556 as an example. For the parameterization of Bernard–Rémond (4), we observe that the parameter α (red curve) has a strong sensitivity for small irradiance values, since α represents the initial slope of the growth rate curve. Moreover, μ_{\max} (blue curve) is the most sensitive parameter when the irradiance approaches x_{opt} , and the sensitivities of α and x_{opt} (yellow curve) go to zero. This is related to the partial derivatives $\partial\mu^4/\partial\theta_j^4$. Indeed, when x approaches x_{opt} , the partial derivatives $\partial\mu^4/\partial\alpha$, $\partial\mu^4/\partial x_{\text{opt}}$ are both close to 0 and $\partial\mu^4/\partial\mu_{\max}$ is close to 1. Thus, μ_{\max} is the most sensitive parameter around x_{opt} . When moving to large values of irradiance, we observe that x_{opt} becomes more sensitive than the other two parameters.

The behavior of the parameterizations of Andrews (1) and Edwards (2) are rather similar. We observe that the parameter $\hat{\mu}$ and μ_m (blue curve) are relatively sensitive along with the irradiance, the sensitivity of the parameter K_x (red curve) decreases as the irradiance increases, and the sensitivity of the parameter K_i (yellow curve) increases as the irradiance decreases, which is in line with the structure of this parameterization, where K_x dominates the numerator at low light and x^2/K_i at high light.

For the parameterization of Peeters–Eilers (3), we observe that the parameter c (yellow curve) is relatively sensitive only for small irradiance values, the sensitivity of the parameter a (blue curve) increases as the irradiance increases, and the sensitivity curve of the parameter b (red curve) shares the same shape as the growth rate. Recall that the parameter c is related to the initial slope of the growth rate, which explains its sensitivity only for small irradiance values.

Regarding our parameterization KIS (5), we observe that the sensitivity curves of

the parameters γ_{\max} and x^* are rather symmetric, with a horizontal symmetrical axis at 0.5. The parameter x^* represents the value for which growth is maximum, and γ_{\max} is proportional to the maximum growth rate. The roles of both parameters are well-balanced, and they share equally the task of representing the growth rate with respect to the irradiance. Moreover, we find that α in the parameterization of Bernard-Rémond (4) is only sensitive for small irradiance, μ_{\max} and x_{opt} rather dominate separately for the rest part. This actually confirms the behavior of our parameterization, as γ_{\max} is very related to μ_{\max} and x^* to x_{opt} . By well choosing these two parameters using their equivalent relationship, our parameterization KIS (5) can very efficiently capture the growth rate.

Similar observations are obtained for the other seven tested species, and their normalized sensitivity curves are illustrated in Fig. B.9 - B.16 in [S2 Appendix](#) for the sake of compactness. Once again, we are able to show the normalized sensitivity curves of the parameterization of Edwards (2) for only two species *Platymonius subcordiformis* and *Chlorococcum sp.* FACHB-1556 due to its identifiability issue.

Conclusion

In this study, we have reviewed and examined four parameterizations (1)-(4) of the Haldane model existing in the literature. We have also introduced a new parameterization KIS (5) based on only two parameters. The parameterization of Edwards (2), even if it has been used in the literature, has serious identifiability problems that lead to disastrous numerical consequences. The parameterizations of Andrews (1) and Peeters-Eilers (3) exhibit a strong correlation between the parameters and the subsequent poor prediction accuracy. The parameterization of Bernard-Rémond (4), which efficiently uncorrelates the three parameters, is the most efficient representation with three parameters. Surprisingly, our two-parameter parameterization KIS (5) out-competes all the other models.

This conclusion on the capability of the parameterization KIS (5) to accurately represent the inhibition of photosynthetic organisms by high light would need to be verified with other cases of growth inhibition (volatile fatty acids, ethanol, phenol, etc.). It perfectly illustrates the principle of "Keep It Simple (KIS)", which should guide the modelling [34]. With fewer parameters, the identification procedure is more efficient, and eventually the modelling uncertainty is better contained than a more complex model, which pay the price of having more parameters.

References

- Spolaore P, Joannis-Cassan C, Duran E, Isambert A. Commercial applications of microalgae. Journal of Bioscience and Bioengineering. 2006;101(2):87–96. doi:10.1263/jbb.101.87.
- Becker EW. Micro-algae as a source of protein. Biotechnology Advances. 2007;25(2):207–210. doi:10.1016/j.biotechadv.2006.11.002.
- Kent M, Welladsen HM, Mangott A, Li Y. Nutritional Evaluation of Australian Microalgae as Potential Human Health Supplements. PLOS ONE. 2015;10(2):1–14. doi:10.1371/journal.pone.0118985.
- Wang Y, Tibbetts SM, McGinn PJ. Microalgae as Sources of High-Quality Protein for Human Food and Protein Supplements. Foods. 2021;10(12). doi:10.3390/foods10123002.

5. Jagadevan S, Banerjee A, Banerjee C, Guria C, Tiwari R, Baweja M, et al. Recent developments in synthetic biology and metabolic engineering in microalgae towards biofuel production. *Biotechnol Biofuels*. 2018;11. doi:10.1186/s13068-018-1181-1.
6. Mata TM, Martins AA, Caetano NS. Microalgae for biodiesel production and other applications: A review. *Renewable and Sustainable Energy Reviews*. 2010;14(1):217–232. doi:10.1016/j.rser.2009.07.020.
7. Zibarev N, Toumi A, Politaeva N, Iljin I. Nutrients recovery from dairy wastewater by Chlorella vulgaris and comparison of the lipid's composition with various chlorella strains for biodiesel production. *PLOS ONE*. 2024;19(4):1–13. doi:10.1371/journal.pone.0297464.
8. Taher H, Al-Zuhair S, Al-Marzouqi A, Haik Y, Farid M. Growth of microalgae using CO₂ enriched air for biodiesel production in supercritical CO₂. *Renewable Energy*. 2015;82:61–70. doi:10.1016/j.renene.2014.08.013.
9. Arora AS, Nawaz A, Qyyum MA, Ismail S, Aslam M, Tawfik A, et al. Energy saving anammox technology-based nitrogen removal and bioenergy recovery from wastewater: Inhibition mechanisms, state-of-the-art control strategies, and prospects. *Renewable and Sustainable Energy Reviews*. 2021;135:110126. doi:/10.1016/j.rser.2020.110126.
10. Edwards VH. The influence of high substrate concentrations on microbial kinetics. *Biotechnology and Bioengineering*. 1970;12(5):679–712. doi:10.1002/bit.260120504.
11. Bernard O, Rémond B. Validation of a simple model accounting for light and temperature effect on microalgal growth. *Bioresource Technology*. 2012;123:520–527. doi:10.1016/j.biortech.2012.07.022.
12. Ucun H, Yildiz E, Nuhoglu A. Phenol biodegradation in a batch jet loop bioreactor (JLB): Kinetics study and pH variation. *Bioresource Technology*. 2010;101(9):2965–2971. doi:10.1016/j.biortech.2009.12.005.
13. Jimenez J, Latrille E, Harmand J, Robles A, Ferrer J, Gaida D, et al. Instrumentation and control of anaerobic digestion processes: a review and some research challenges. *Reviews in Environmental Science and Bio/Technology*. 2015;14:615–648. doi:10.1007/s11157-015-9382-6.
14. Bernard O, Lu LD. Optimal optical conditions for Microalgal production in photobioreactors. *Journal of Process Control*. 2022;112:69–77. doi:10.1016/j.jprocont.2022.03.001.
15. Lee E, Jalalizadeh M, Zhang Q. Growth kinetic models for microalgae cultivation: A review. *Algal Research*. 2015;12:497–512. doi:10.1016/j.algal.2015.10.004.
16. Monod J. Recherches sur la croissance des cultures bactériennes [Thèse de doctorat Sciences naturelles]. Université de Paris. Paris; 1941.
17. Jannasch HW, Egli T. Microbial growth kinetics: a historical perspective. *Antonie van Leeuwenhoek*. 1993;63:213–224. doi:10.1007/BF00871219.
18. Hsu SB, Waltman P. A survey of mathematical models of competition with an inhibitor. *Mathematical Biosciences*. 2004;187(1):53–91. doi:10.1016/j.mbs.2003.07.004.

19. Andrews JF. A mathematical model for the continuous culture of microorganisms utilizing inhibitory substrates. *Biotechnology and Bioengineering*. 1968;10(6):707–723. doi:10.1002/bit.260100602.
20. Haldane JBS. Enzymes. London: Longmans, Green & Co.; 1930.
21. D'Adamo PD, Rozich AF, Jr AFG. Analysis of Growth Data with Inhibitory Carbon Sources. *Biotechnology and Bioengineering*. 1984;26:397–402. doi:10.1002/bit.260260421.
22. Han K, Levenspiel O. Extended Monod Kinetics for Substrate, Product, and Cell Inhibition. *Biotechnology and Bioengineering*. 1988;32:430–437. doi:10.1002/bit.260320404.
23. Reardon KF, Mosteller DC, Bull Rogers JD. Biodegradation kinetics of benzene, toluene, and phenol as single and mixed substrates for *Pseudomonas putida* F1. *Biotechnology and Bioengineering*. 2000;69(4):385–400. doi:10.1002/1097-0290(20000820)69:4:385::AID-BIT5;3.0.CO;2-Q.
24. Banerjee A, Ghoshal AK. Phenol degradation by *Bacillus cereus*: pathway and kinetic modeling. *Bioresource Technology*. 2010;101(14):5501–5507. doi:10.1016/j.biortech.2010.02.018.
25. García-Díéguez C, Bernard O, Roca E. Reducing the Anaerobic Digestion Model No. 1 for its application to an industrial wastewater treatment plant treating winery effluent wastewater. *Bioresource technology*. 2013;132:244–253. doi:10.1016/j.biortech.2012.12.166.
26. Kok B. On the inhibition of photosynthesis by intense light. *Biochimica et Biophysica Acta*. 1956;21(2):234–244. doi:10.1016/0006-3002(56)90003-8.
27. Peeters JCH, Eilers PHC. The relationship between light intensity and photosynthesis—A simple mathematical model. *Hydrobiological Bulletin*. 1978;12(2):134–136. doi:10.1007/BF02260714.
28. Aiba S. Growth kinetics of photosynthetic microorganisms. In: Microbial Reactions. vol. 23. Springer Berlin Heidelberg; 1982. p. 85–156.
29. Eilers PHC, Peeters JCH. A model for the relationship between light intensity and the rate of photosynthesis in phytoplankton. *Ecological Modelling*. 1988;42:199–215. doi:10.1016/0304-3800(88)90057-9.
30. Talbot P, Thébault JM, Dauta A, Noüe JDL. A comparative study and mathematical modeling of temperature, light and growth of three microalgae potentially useful for wastewater treatment. *Water Research*. 1991;25(4):465–472. doi:10.1016/0043-1354(91)90083-3.
31. Hill GA, Robinson CW. Substrate inhibition kinetics: phenol degradation by *Pseudomonas putida*. *Biotechnology and Bioengineering*. 1975;17(11):1599–1615. doi:10.1002/bit.260171105.
32. Wang SJ, Loh KC. Modeling the role of metabolic intermediates in kinetics of phenol biodegradation. *Enzyme and Microbial Technology*. 1999;25(3-5):177–184. doi:10.1016/S0141-0229(99)00060-5.
33. Boon B, Laudelout H. Kinetics of Nitrite Oxidation by *Nitrobacter winogradskyi*. *Biochemical Journal*. 1962;85(3):440–447. doi:10.1042/bj0850440.

34. Mairet F, Bernard O. Twelve quick tips for designing sound dynamical models for bioprocesses. *PLoS Computational Biology*. 2019;15(8):e1007222. doi:10.1371/journal.pcbi.1007222.
35. Anning T, MacIntyre HL, Pratt SM, Sammes PJ, Gibb S, Geider RJ. Photoacclimation in the marine diatom *Skeletonema costatum*. *Limnology and Oceanography*. 2000;45(8):1807–1817. doi:10.4319/lo.2000.45.8.1807.
36. Yang XL, Liu LH, Yin ZK, Wang XY, Wang SB, Ye ZP. Quantifying photosynthetic performance of phytoplankton based on photosynthesis–irradiance response models. *Environmental sciences Europe*. 2020;32(1). doi:10.1186/s12302-020-00306-9.
37. James G, Witten D, Hastie T, Tibshirani R. An introduction to statistical learning. Springer; 2013.
38. Chatterjee S, Hadi AS. Regression Analysis by Example. Wiley Series in Probability and Statistics. Wiley; 2006.
39. Lagarias JC, Reeds JA, Wright MH, Wright PE. Convergence properties of the Nelder–Mead simplex method in low dimensions. *SIAM Journal on optimization*. 1998;9(1):112–147. doi:10.1137/S1052623496303470.
40. van Impe JF, Vanrolleghem PA, Iserentant DM, editors. Advanced Instrumentation, Data Interpretation, and Control of Biotechnological Processes. Springer Netherlands; 1998.
41. Casagli F, Rossi S, Steyer JP, Bernard O, Ficara E. Balancing microalgae and nitrifiers for wastewater treatment: can inorganic carbon limitation cause an environmental threat? *Environmental science & technology*. 2021;55(6):3940–3955. doi:10.1021/acs.est.0c05264.
42. Cariboni J, Gatelli D, Liska R, Saltelli A. The role of sensitivity analysis in ecological modelling. *Ecological Modelling*. 2007;203(1):167–182. doi:10.1016/j.ecolmodel.2005.10.045.
43. Kenneth PB, David RA, editors. Model Selection and Multimodel Inference. Springer-Verlag New York; 1998.
44. Burnham KP, Anderson DR, P HK. AIC model selection and multimodel inference in behavioral ecology: some background, observations, and comparisons. *Behavioral ecology and sociobiology*. 2011;65(1):23–35. doi:10.1007/s00265-010-1029-6.
45. McQuarrie ADR, Tsai CL. Regression and Time Series Model Selection. World Scientific; 1998.
46. Burnham KP, Anderson DR. Multimodel Inference: Understanding AIC and BIC in Model Selection. *Sociological Methods and Research*. 2004;33(2):261–304. doi:10.1177/0049124104268644.

Supporting information

S1 Appendix. Figures for prediction intervals.

S2 Appendix. Figures for normalized sensitivity.

Introduction

Microorganisms, such as bacteria, cyanobacteria, microalgae, or yeast, have tremendous potential for a wide range of applications. Due to their simple cellular structure, they can be grown quickly and efficiently in bioreactors, for pollution removal, feed or food production, and for the production of high value-added products in the chemical industry [1, 2, 3, 4]. Additionally, various microorganisms offer avenues for the production of biofuels, using their potential to store lipids and carbohydrates that can be converted to biodiesel and ethanol [5, 6, 7]. Photosynthetic microorganisms (cyanobacteria and microalgae) can even contribute to the fixation of CO₂ and its transformation into valuable products for green chemistry or for the production of biofuels [8]. A common problem for many of these applications is the drop in process efficiency when one of the compounds, typically a substrate, is in excess and becomes an inhibitor, such as for ammonium [9], sodium [10], light [11] or phenol [12]. Models that support advanced control strategies can be the cornerstone of better managing inhibition [13, 14]. However, the models that represent growth at low concentration and then inhibition present some technical issues that make their calibration difficult, and this is the main focus of this paper.

There exists a broad range of mathematical models that can represent the growth kinetics of microorganisms as a function of the main factors affecting their metabolism. We refer to [15] for a brief review of some widely used models. Among them, the Monod model, introduced by J. Monod in [16], is probably the most famous kinetic model due to its simple formula and its ability to represent substrate-limited microbial growth [17, 18]. However, as J.F. Andrews later pointed out in [19]:

..., the Monod relationship cannot be valid for those substrates which limit growth at low concentrations and are inhibitory to the organism at higher concentrations.

To account for inhibition at high substrate concentrations, Andrews proposed in [19] the use of the Haldane model [20], initially developed by J.B.S. Haldane to represent enzymes inhibition by high substrate concentrations, to describe the microbial growth kinetics. In particular, it was noted:

Although there is no theoretical basis for the use of this function for microorganisms, it should be pointed out that the Monod relationship, which is empirical, is similar in form to the Michaelis-Menton expression upon which the Haldane function is based.

Since then, the Haldane model has become one of the most popular approaches to represent substrate inhibition in microbial growth kinetics. It shows a reasonable fit to experimental data for various species [19, 10, 21, 22], and it also finds numerous applications for substrates that can become inhibitory, such as phenol, ethanol, or volatile fatty acids [23, 24, 12, 25]. In another class of applications, inhibitory effects on photosynthesis have been observed after exposure to strong light intensities, causing specific damage occurs to photosynthetic units, as discussed by B. Kok in [26]:

If algae are exposed to very strong light, the maximum photosynthetic rate does not persist; sooner or later it decreases and may ultimately drop to zero.

To account for this phenomenon of photoinhibition, the Haldane model has been used to describe the effect of excess light on photosynthetic microorganisms, and its effectiveness has also been validated experimentally [27, 28, 29, 30, 11].

Despite the widespread use of the Haldane model to represent inhibitory effects, its practical application often proves intricate due to the variety of parameterizations proposed in the literature [19, 10, 27, 11]. Mathematically, this model can be expressed as the ratio of a term proportional to the substrate concentration (or the light intensity) and a second-order polynomial. In other words, the inverse of the yield (ratio of the factor to the growth rate) is a quadratic polynomial. Although numerous parameterizations of the Haldane model have been proposed, it can be shown that they are actually mathematically equivalent. This then raises three main questions.

- Q1. Which parameterizations are preferable in terms of parameter identifiability process and resulting model accuracy ?
- Q2. Are there alternative equivalent parameterizations that are easier to estimate and can provide higher accuracy ?
- Q3. How can different parameterizations of a same model be calibrated and systematically compared ?

To the best of our knowledge, no systematic study has yet addressed these questions. Therefore, we aim to provide such an analysis in this paper.

The current study is organized as follows. We first review existing parameterizations in the literatures and show their mathematical equivalence. Meanwhile, we present a new equivalent parameterization requiring fewer parameters. We then restrict to a single inhibitory effect in order to investigate the identification and calibration properties of these parameterizations. The sources of experimental data and the methods used in our analyses are then described. To select the best parameterization, we compare results obtained using standard model selection criteria with those derived from a new enhanced criterion. Finally, we present some numerical experiments and conclude with a detailed discussion with some comments on the findings of our studies.

Mathematical analysis

Generally speaking, parameterizations of the Haldane are not always presented consistently in the literature, and the use of different parameterizations can sometimes be misleading. To address this, we briefly provide a historical review of the four major parameterizations of the Haldane model to describe microbial growth kinetics, and then analyze mathematically their relationship.

Historical review

The original model was introduced by J.B.S. Haldane in 1930 in the context of enzymes kinetics [20], and it was first adapted by J.F. Andrews in 1968 for microbial growth under substrate inhibition in [19]. Thus, the model is often referred to as the Haldane–Andrews model in the context of microbial growth kinetics. This model uses three parameters to describe the growth kinetics:

$$\mu^2(x) = \frac{\hat{\mu}}{1 + \frac{K_x}{x} + \frac{x}{K_i}}, \quad (1)$$

where $\hat{\mu}$ is the maximum specific growth rate in the absence of inhibition (inverse of time), K_x is the saturation constant, numerically equals lowest concentration of substrate at which the specific growth rate is equal to one-half the maximum specific growth rate in the absence of inhibition (mass over volume), and K_i is the inhibition constant, numerically equals the highest substrate concentration at which the specific growth rate is equal to one-half the maximum specific growth rate in the absence of inhibition (mass over volume). This parameterization has been well studied and calibrated with experimental data of various species and different substrate inhibitors, e.g., see [31, 21, 32].

In subsequent work, V.H. Edwards in 1970 used a similar notation for another triplet (μ_m, K_x, K_i) in [10] to describe microbial growth kinetics:

$$\mu^4(x) = \frac{\mu_m x}{(x + K_x)(1 + \frac{x}{K_i})}, \quad (2)$$

where the interpretation of each parameter was not explicitly specified. Edwards further claimed in [10] that this equation was also derived by Haldane. However, the two equations (1) and (2) are actually not the same. Dividing both numerator and denominator of (2) by x yields

$$\mu^4(x) = \frac{\mu_m}{(1 + \frac{K_x}{x})(1 + \frac{x}{K_i})} = \frac{\mu_m}{1 + \frac{K_x}{x} + \frac{x}{K_i} + \frac{K_x}{K_i}},$$

which is different from (1). Therefore, despite the same notation K_x and K_i in both parameterizations, their interpretations may not coincide. This ambiguity leads to potential identifiability issue, which will be further discussed in the following. Nevertheless, the use of Edwards-type parameterization can be traced back in 1962 by B. Boon and H. Laudelout [33], who applied it to describe the kinetics of Nitrite oxidation by *Nitrobacter*.

In 1978, J.C.H. Peeters and P.H.C. Eilers proposed in [27] a different parameterization of the Haldane model to describe the photoinhibition effect of microorganisms. They rather use three arbitrary parameters a , b , and c to represent the growth kinetics:

$$\mu^3(x) = \frac{x}{ax^2 + bx + c}. \quad (3)$$

In particular, they noted in [27] that

The parameters values do not follow from the theory; they have to be fitted for real measurements.

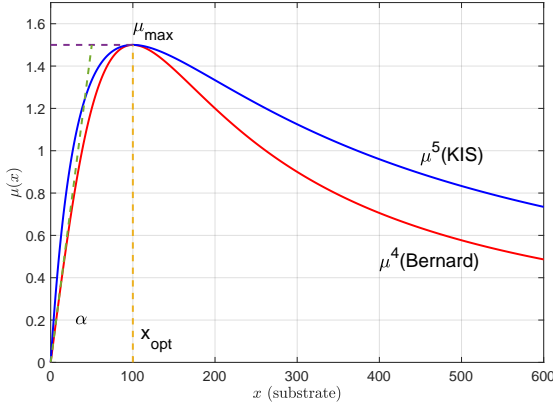


Figure 1: Representation of two Haldane parameterizations. Red curve: parameterization of Bernard and Rémond (4) with the three fundamental parameters, μ_{\max} the maximum growth rate for the optimal irradiance x_{opt} , and α the initial slope. Blue curve: new parameterization KIS (5) with only two parameters γ_{\max} and x^* .

Although the authors did not mention explicitly the Haldane model in [27], their work marks the first attempt to apply this model to describe the relationship between light intensity and photosynthesis, and it has been widely used and calibrated by experimental data, e.g., see [28, 30].

More than three decades later, O. Bernard and B. Rémond proposed in 2012 a new parameterization of the Haldane model in [11] to account for the influence of light on phytoplankton growth rate. This parameterization also contains three parameters given by

$$\mu^1(x) = \frac{\mu_{\max}x}{x + \frac{\mu_{\max}}{\alpha}(\frac{x}{x_{\text{opt}}} - 1)^2}, \quad (4)$$

where μ_{\max} is the maximum growth rate for the optimal irradiance (s^{-1}), α is the initial slope of the light response curve ($\mu\text{mol}^{-1} \text{photons m}^2$), and x_{opt} is the value of the irradiance for which the growth is maximal ($\mu\text{mol photons m}^{-2} \text{s}^{-1}$). One major advantage of this parameterization is the physical meaning of each parameter. Indeed, the growth kinetics for this parameterization is depicted in Fig. 1 (red curve) together with three parameters ($\mu_{\max}, x_{\text{opt}}, \alpha$). We observe that these three parameters are mathematically fundamental to characterize the growth curve. This also allows a better performance in the calibration process, as shown later in our numerical experiments.

Equivalent relationship between parameterizations

As the three parameters $(\mu_{\max}, \alpha, x_{\text{opt}})$ in (4) have a clear physical meaning, and parameters in the other parameterizations do not have a direct interpretation. We use (4) as our reference and $(\mu_{\max}, \alpha, x_{\text{opt}})$ as our fundamental parameters. To show that four equations (1)-(4) are all mathematically equivalent, we rewrite each parameterization in the same form as our reference, and we find,

- parameterization of Andrews (1):

$$\hat{\mu} = \frac{\mu_{\max}\alpha x_{\text{opt}}}{\alpha x_{\text{opt}} - 2\mu_{\max}}, \quad K_x = \frac{\mu_{\max}x_{\text{opt}}}{\alpha x_{\text{opt}} - 2\mu_{\max}}, \quad K_i = \frac{x_{\text{opt}}(x_{\text{opt}}\alpha - 2\mu_{\max})}{\mu_{\max}},$$

with the units of each parameter $\hat{\mu}$ (inverse of time), K_x and K_i (same as x). Note that the parameters of this model are complex combinations of the three fundamental parameters.

- parameterization of Edwards (2):

$$\mu_m = \alpha K_x, \quad K_x K_i = x_{\text{opt}}^2, \quad K_x + K_i = \frac{(\alpha x_{\text{opt}} - 2\mu_{\max})x_{\text{opt}}}{\mu_{\max}},$$

with the unit of μ_m (inverse of time), K_x and K_i the same units as x . Note that there are two (equivalent) possible values for the couple (K_x, K_i) , which illustrates the dramatic identifiability issue of this model in practice, e.g., see [34, Tip 6].

- parameterization of Peeters and Eilers (3):

$$a = \frac{1}{\alpha x_{\text{opt}}^2}, \quad b = \frac{1}{\mu_{\max}} - \frac{2}{\alpha x_{\text{opt}}}, \quad c = \frac{1}{\alpha},$$

with units for b (time), a (time per unit of x) and c (time times unit of x). We observe that the parameter c is directly connected to α , and the parameter a is deduced from α and x_{opt} . The parameter b results from the three fundamental parameters.

This not only shows the equivalent relationship of these four major parameterizations, but also reveals the link between each parameter.

New parameterization: KIS

Each of the four parameterizations (1)-(4) contains three parameters to describe microbial growth kinetics, but one of the main proposes of our work (Q2) is to search for alternative parameterization containing fewer parameters. For this reason, we introduce a new Haldane type parameterization with only two parameters to characterize the growth:

$$\mu^5(x) = 4\gamma_{\max} \frac{xx^*}{(x+x^*)^2}. \quad (5)$$

Before presenting the physical meaning of these two parameters γ_{\max} and x^* , we first show that (5) is also equivalent to other parameterizations. Once again, we rewrite (5) in the form of (4), we obtain directly

$$\gamma_{\max} = \mu_{\max}, \quad x^* = x_{\text{opt}}, \quad \frac{4\gamma_{\max}}{x^*} = \alpha.$$

Mathematically speaking, the parameters (γ_{\max}, x^*) are exactly the same to $(\mu_{\max}, x_{\text{opt}})$ as long as they satisfy $4\gamma_{\max}/x^* = \alpha$. Furthermore, the parameter x^* (same unit as x) corresponds to the value of x for which the growth rate is the maximum, and the parameter γ_{\max} (inverse of time) is the maximum growth rate obtained for x^* . Indeed, the growth curve using this new parameterization is also illustrated in Fig. 1 (blue curve). Although (γ_{\max}, x^*) and $(\mu_{\max}, x_{\text{opt}})$ seem very similar in Fig. 1, their values are chosen differently such that $4\frac{\gamma_{\max}}{x^*} \neq \alpha$, which helps to distinguish the two curves. We observe that this new parameterization of the Haldane model with only two parameters can also well represent the growth kinetics with inhibition effect. Furthermore, each parameter has a clear physical interpretation, which shows great advantage in the calibration process and sensitivity analysis, as discussed in our numerical experiments. From a modelling perspective, a model with fewer parameters but still captures the essential features of the phenomenon is generally preferable. This two-parameter formulation (5) follows exactly this spirit and provides a new idea of modelling inhibitory effect: Keep It Simple (KIS).

Materials and methods

All five parameterizations (1)-(5) are mathematically equivalent one to the other, the only difference is from the calibration and identification viewpoint. To study the identifiability and eventually select the best parameterization (Q1), we focus on the specific inhibition example of microalgae kinetics growth with respect to the irradiance. From now on, the variable x in (1)-(5) represents the irradiance with the unit ($\mu\text{mol photons m}^{-2} \text{s}^{-1}$). We assess the uncertainty associated with the parameterization predictions and identify the most appropriate parameter values of each parameterization for the given experimental conditions.

Experimental data

The experimental data are taken from the literature [35, 36] that contains in total eight different microalgae species. For self-completeness, we briefly describe these experiments.

Growth response with *Skeletonema costatum*

Anning et al. [35] study the growth of the diatom *Skeletonema costatum* strain CCMP 1332 (Plymouth Culture Collection). The algae cells are cultured under the same conditions, except for the irradiance levels. Here, we focus on the curve obtained for the pre-acclimation at $1200 \mu\text{mol photons m}^{-2} \text{s}^{-1}$, for which the photoinhibition is more marked. Labelled $\text{NaH}^{14}\text{CO}_3$ was used to culture algal cells simultaneously over a gradient of irradiance to determine photosynthetic carbon fixation.

Growth response via oxymetry for seven species of phytoplankton

Yang et al. [36] investigate the photosynthetic response of seven strains of phytoplankton, comprising three strains of marine phytoplankton (*Isochrysis galbana*, *Dunaliella salina*, and *Platymonas subcordiformis*) and four strains of freshwater phytoplankton (*Chlorococcum sp.* FACHB-1556, *Microcystis aeruginosa* FACHB-905, *Microcystis wesenbergii* FACHB-1112, and *Scenedesmus obliquus* FACHB-116.). Cells are cultured at an irradiance of $60 \mu\text{mol photons m}^{-2} \text{s}^{-1}$ for 12 hours per day and at a temperature of $26 \pm 1^\circ\text{C}$ for 7 to 10 days. The cells are then subjected to increasing levels of irradiance, ranging from 0 to $1200 (\mu\text{mol photons m}^{-2} \text{s}^{-1})$, provided by a digital LED light source at a temperature of $25 \pm 1^\circ\text{C}$. The oxygen-evolving rate is measured by using dissolved oxygen measurements.

Parameter identification

To identify appropriate parameterizations from the experimental data, we need to introduce some notations. Let us denote by θ^k the parameter set corresponding to the parameterization μ^k :

$$\begin{aligned}\theta^2 &= (\hat{\mu}, K_x, K_i) \text{ for } \mu^2 \text{ in (1), } \theta^4 = (\mu_m, K_x, K_i) \text{ for } \mu^4 \text{ in (2), } \theta^3 = (a, b, c) \text{ for } \mu^3 \text{ in (3),} \\ \theta^1 &= (\mu_{\max}, \alpha, x_{\text{opt}}) \text{ for } \mu^1 \text{ in (4), } \theta^5 = (\gamma_{\max}, x^*) \text{ for } \mu^5 \text{ in (5).}\end{aligned}$$

We denote by m the number of parameters and by θ_j^k ($j = 1, \dots, m$) each element of the parameter set θ^k . For instance, $\theta_1^1 = \mu_{\max}$, $\theta_2^1 = \alpha$, and $\theta_3^1 = x_{\text{opt}}$ in (4). Note that $m = 3$ for parameterizations (1)-(4), and $m = 2$ for the parameterization (5). For each microalgae species, we denote by $(x_i)_{i=1}^n$ the irradiance samples (with n the size of the samples) and $\mu_{\text{exp}}(x_i)$ the associated experimental estimations of the growth rate. We denote by $\mu^k(x_i, \theta^k)$ the growth rate evaluated in the light sample x_i using the parameterization μ^k . The sum of the squared error (SSE) [37, 38] is given by:

$$\text{SSE} := \sum_{i=1}^n (\mu_{\text{exp}}(x_i) - \mu^k(x_i, \theta^k))^2. \quad (6)$$

With this, for each parameterization μ^k , the parameter identification problem can be stated as a standard nonlinear least-squares optimization problem:

$$\begin{aligned}\min_{\theta^k} \quad & \text{SSE} = \sum_{i=1}^n (\mu_{\text{exp}}(x_i) - \mu^k(x_i, \theta^k))^2, \\ \text{subject to} \quad & \theta_{\min}^k \leq \theta^k \leq \theta_{\max}^k,\end{aligned} \quad (7)$$

where $[\theta_{\min}^k, \theta_{\max}^k]$ is an appropriate theoretical range of the parameter values. A parameter set θ^k that solves this optimization problem is a local optimal parameter set. Since the uniqueness of the optimum is not guaranteed, we choose the best parameter set as the local optimum for which the SSE value is the smallest. Numerically, we use the Nelder–Mead simplex algorithm [39] implemented in the *fminsearch* function of Matlab.

Sensitivity analysis

Once the best parameter set θ^k has been identified, we compute the sensitivity equations to determine the Fisher information matrix (FIM) to compare different parameterizations [40]. The FIM is defined by,

$$F := \left(\frac{\partial \mu^k}{\partial \theta^k}(x) \right)^T Q \frac{\partial \mu^k}{\partial \theta^k}(x), \quad (8)$$

where Q is a square matrix representing the inverse of the covariance matrix of the measurement error. This information was not provided for $\mu_{\text{exp}}(x_i)$ in the considered experimental data. We therefore assumed a 10% standard variation for each measurement, except for the lowest values where this value is saturated at a minimum level, following the strategy of [41]. More formally, we assume that the standard variation vector is:

$$W := \max_{i=1, \dots, n} \left(0.1 \mu_{\text{exp}}(x_i), 0.02 \max_{i=1, \dots, n} (\mu_{\text{exp}}(x_i)) \right). \quad (9)$$

We then define Q as a diagonal matrix with the entries $Q_{ii} := 1/W_i^2$.

For each parameter set θ^k , the standard deviation is defined by

$$\sigma := s \sqrt{n \text{diag}(V)}, \quad (10)$$

where $V := F^{-1}$ is the covariance matrix of parameter estimation error, and s is the residual mean square with:

$$s^2 := \frac{\sum_{i=1}^n (\mu^k(x_i, \theta^k) - \mu_{\text{exp}}(x_i))^T Q_i (\mu(x_i, \theta^k) - \mu_{\text{exp}}(x_i))}{n - m}. \quad (11)$$

From the parameter standard deviation, we can compute the prediction interval (PI) by

$$PI := \mu^k \pm Z e, \quad (12)$$

where Z is the value of Student's t -distribution choosing a significance level 0.05, and e is the error propagation with $e := \sqrt{\sum_{j=1}^m (\frac{\partial \mu^k}{\partial \theta_j^k})^2 \sigma_j^2}$. The adequacy of the parameterization μ^k with the experimental measurements is the first criterion to assess its performance.

Additionally, the sensitivity of the parameter θ_j^k is computed as the normalized sensitivity [42]

$$S_j := \left(\frac{\sigma_j}{e} \frac{\partial \mu^k}{\partial \theta_j^k} \right)^2. \quad (13)$$

Parameterization selection criteria: PEMAC

The most popular model selection criteria are Akaike's information criterion (AIC) [43, 44, 37] and Bayesian information criterion (BIC) [45, 46]. They are used in the analysis of empirical data that account for the differences in the model degrees of freedom. By comparing the AIC and BIC values and the identification results, we can determine the best model. We recall here the definition of AIC

$$\text{AIC} := n \log\left(\frac{\text{SSE}}{n}\right) + 2(m + 1). \quad (14)$$

For small-samples, when $\frac{n}{m+1} < 40$, the AIC becomes the corrected Akaike information criterion (AIC_c), given by :

$$\text{AIC}_c := \text{AIC} + \frac{2(m + 1)(m + 2)}{n - m - 2}. \quad (15)$$

The Bayesian information criterion is given by:

$$\text{BIC} := n \log\left(\frac{\text{SSE}}{n}\right) + (m + 1) \log(n). \quad (16)$$

Both criteria have been proven to be very effective when comparing and selecting different *models*. However, they become less efficient when it comes to distinguishing equivalent parameterizations of the *same model*. To address this issue (Q3), we introduce a new criterion based on the criteria AIC_c and BIC to improve the sensitivity to evaluate various parameterizations of one model. Let us denote by \bar{e} the average of the error propagation e , which is an important criterion for qualifying the model accuracy

$$\bar{e} := \frac{1}{n} \sum_{i=1}^n \sqrt{\sum_{j=1}^m \left(\frac{\partial \mu^k}{\partial \theta_j^k}(x_i) \right)^2 \sigma_j^2}. \quad (17)$$

The new criterion, namely the Propagated Error Modified Akaike Criterion (PEMAC), is defined by

$$\text{PEMAC} := \begin{cases} 2n \log(\bar{e}) + n \log\left(\frac{\text{SSE}}{n}\right) \\ \quad + (m + 1) \log n, & \frac{n}{m + 1} \geq 40, \\ 2n \log(\bar{e}) + n \log\left(\frac{\text{SSE}}{n}\right) \\ \quad + \frac{2(m + 1)(m + 2)}{n - m - 2}, & \frac{n}{m + 1} < 40. \end{cases}$$

We will compare our criterion with AIC_c and BIC , and show that our criterion provides better performance in terms of selecting the best parameterizations of the same model.

		1	2	3	4	5	6	7	8
(1)	$\hat{\mu}$	3.1756×10^{-4}	0.9330	0.1050	0.0518	0.0458	-1.9147	11.9335	1.5156
	K_x	3504.5484	9240.9056	398.3028	69.4167	138.2674	-3875.0132	30429.2456	4324.3801
	K_i	265.8140	52.6380	484.0769	922.3136	848.7246	-29.7342	3.3641	54.3864
SSE		1.1164×10^{-10}	1.2346×10^{-5}	1.0841×10^{-5}	4.6218×10^{-5}	1.0985×10^{-5}	6.0475×10^{-5}	3.5333×10^{-5}	3.1000×10^{-5}
(2)	μ_m	1.5234×10^{-4}	0.1318	0.1449	0.0565	0.0576	0.3138	0.2241	0.2989
	K_x	1273.9800	914.5639	458.7265	75.6161	173.8978	343.2328	323.1022	544.4024
	K_i	1274.3248	914.5640	458.7265	846.6974	674.8267	343.2328	323.1022	544.4024
SSE		1.5685×10^{-10}	4.3482×10^{-5}	2.0970×10^{-5}	4.6218×10^{-5}	1.0985×10^{-5}	6.0296×10^{-4}	2.8402×10^{-4}	3.0619×10^{-4}
(3)	a	11.8466	0.0204	0.0197	0.0209	0.0257	0.0176	0.0249	0.0121
	b	3148.9876	1.0718	9.5276	19.2887	21.8174	-0.5223	0.0838	0.6598
	c	1.1036×10^7	9904.8464	3794.8752	1338.9598	3016.6396	2023.8331	2549.9064	2853.2691
SSE		1.1164×10^{-10}	1.2346×10^{-5}	1.0841×10^{-5}	4.6218×10^{-5}	1.0985×10^{-5}	6.0475×10^{-5}	3.5333×10^{-5}	3.1000×10^{-5}
(4)	μ_{\max}	3.8436×10^{-5}	0.0339	0.0373	0.0335	0.0254	0.0877	0.0624	0.0805
	α	9.0614×10^{-8}	1.0096×10^{-4}	2.6351×10^{-4}	7.4685×10^{-4}	3.3149×10^{-4}	4.9411×10^{-4}	3.9217×10^{-4}	3.5048×10^{-4}
	x_{opt}	965.1726	697.4415	439.1005	253.0296	342.5652	339.4417	319.9471	484.9611
SSE		1.1164×10^{-10}	1.2346×10^{-5}	1.0841×10^{-5}	4.6218×10^{-5}	1.0985×10^{-5}	6.0475×10^{-5}	3.5333×10^{-5}	3.1000×10^{-5}
(5)	γ_{\max}	3.8086×10^{-5}	0.0329	0.0362	0.0351	0.0257	0.0784	0.0560	0.0747
	x^*	1273.9800	914.5640	458.7265	248.7247	338.0766	343.2328	323.1022	544.4024
SSE		1.5685×10^{-10}	4.3482×10^{-5}	2.0970×10^{-5}	6.8655×10^{-5}	1.2139×10^{-5}	6.0296×10^{-4}	2.8402×10^{-4}	3.0619×10^{-4}

Table 1: Best estimates of five parameterizations (1)-(5) for each microalgae species. (1: *Skeletonema costatum*, 2: *Isochrysis galbana*, 3: *Dunaliella salina*, 4: *Platymonas subcordiformis*, 5: *Chlorococcum sp.* FACHB-1556, 6: *Microcystis aeruginosa* FACHB-905, 7: *Microcystis wesenbergii* FACHB-1112, 8: *Scenedesmus obliquus* FACHB-116.)

Results

We now compare numerical performance of the four existing parameterizations (1)-(4) and our new parameterization (5). Our analyses are based on the experimental data for the light response of eight different microalgae species. For each species, we identify the most appropriate parameter values, present the sensitivity and the identifiability of each parameterization.

Parameter identification results

For each parameterization μ^k among (1)-(5), the optimal parameter set θ^k varies under different experimental conditions and different microalgae species. Table 1 presents the optimal parameter sets and the SSE values for each parameterization and for eight microalgae species. The SSE values for the species *Skeletonema costatum* is smaller not only due to the quality of the fit, but also because the measurement method is different, and with different units. This also reflects on the identified parameter values, e.g., the value obtained for μ_{\max} is 3.8436×10^{-5} with the unit s^{-1} , but h^{-1} for the rest. Regarding the seven other species, the SSE values are on the scale of 10^{-5} , except for the parameterizations of Edwards (2) and KIS (5) with the species *Microcystis wesenbergii* FACHB-1112, *Scenedesmus obliquus* FACHB-116 and *Chlorococcum sp.* FACHB-1556, where the SSE values are on the scale of 10^{-4} . This reveals that the parameterizations of Andrews (1), Peeters (3) and Bernard (4) in their identified parameter sets fit slightly better the experimental data in [36] compared to Edwards (2) and KIS (5). Although the parameterization of Bernard (4) is specifically designed to study the influence of irradiance on phytoplankton growth rate, we observe that there are no great differences in its SSE values with the other four parameterizations. This is not surprising since the underlying mathematical model is identical, and only the way the parameters are expressed is changing. Moreover, we observe that, in general, the identified values of γ_{\max} and x^* in KIS (5) are quite similar to μ_{\max} and x_{opt} in Bernard (4). This further confirms the physical meaning of the two parameters in the proposed new parameterization (5). For the following numerical tests, we will use the optimal parameter values given in Table 1.

Correlation matrix of parameter estimation error

Based on the covariance matrix of the parameter estimation error V , we compute the correlation matrix of the parameter estimation error, and illustrate in Table 2 for all five parameterizations and eight microalgae species. We consider that two parameters θ_i^k and θ_j^k are correlated if the absolute value of their correlation exceeds 0.9. Taking this into account, we observe that the three fundamental parameters $(\mu_{\max}, \alpha, x_{\text{opt}})$ in the parameterization of Bernard (4) are rather uncorrelated with each other, and same observation goes for the two parameters (γ_{\max}, x^*) in the parameterization KIS (5). On the other hand, the three parameters $(\hat{\mu}, K_x, K_i)$ in the parameterization of

	1			2			3			4			5			6			7			8		
(1)	$\hat{\mu}$	K_x	K_i	$\hat{\mu}$	K_x	K_i	$\hat{\mu}$	K_x	K_i	$\hat{\mu}$	K_x	K_i	$\hat{\mu}$	K_x	K_i	$\hat{\mu}$	K_x	K_i	$\hat{\mu}$	K_x	K_i	$\hat{\mu}$	K_x	K_i
$\hat{\mu}$	1.00	1.00	-1.00	1.00	1.00	-1.00	1.00	0.99	-0.99	1.00	0.93	-0.95	1.00	0.96	-0.96	1.00	1.00	-1.00	1.00	1.00	-1.00	1.00	1.00	-1.00
K_x	1.00	1.00	-1.00	1.00	1.00	-1.00	0.99	1.00	-0.97	0.93	1.00	-0.86	0.96	1.00	-0.91	1.00	1.00	-1.00	1.00	1.00	-1.00	1.00	1.00	-1.00
K_i	-1.00	-1.00	1.00	-1.00	-1.00	1.00	-0.99	-0.97	1.00	-0.95	-0.86	1.00	-0.96	-0.91	1.00	-1.00	-1.00	1.00	-1.00	-1.00	1.00	-1.00	1.00	-1.00
(2)	μ_m	K_x	K_i	μ_m	K_x	K_i	μ_m	K_x	K_i	μ_m	K_x	K_i	μ_m	K_x	K_i	μ_m	K_x	K_i	μ_m	K_x	K_i	μ_m	K_x	K_i
μ_m	-	-	-	-	-	-	-	-	-	1.00	0.96	-0.97	1.00	0.99	-0.99	-	-	-	-	-	-	-	-	-
K_x	-	-	-	-	-	-	-	-	-	0.96	1.00	-0.91	0.99	1.00	-0.97	-	-	-	-	-	-	-	-	-
K_i	-	-	-	-	-	-	-	-	-	-0.97	-0.91	1.00	-0.99	-0.97	1.00	-	-	-	-	-	-	-	-	-
(3)	a	b	c	a	b	c	a	b	c	a	b	c	a	b	c	a	b	c	a	b	c	a	b	c
a	1.00	-0.95	0.72	1.00	-0.94	0.72	1.00	-0.90	0.62	1.00	-0.87	0.55	1.00	-0.89	0.58	1.00	-0.91	0.69	1.00	-0.90	0.64	1.00	-0.92	0.70
b	-0.95	1.00	-0.85	-0.94	1.00	-0.86	-0.90	1.00	-0.79	-0.87	1.00	-0.72	-0.89	1.00	-0.74	-0.91	1.00	-0.86	-0.90	1.00	-0.83	-0.92	1.00	-0.85
c	0.72	-0.85	1.00	0.72	-0.86	1.00	0.62	-0.79	1.00	0.55	-0.72	1.00	0.58	-0.74	1.00	0.69	-0.86	1.00	0.64	-0.83	1.00	0.70	-0.85	1.00
(4)	μ_{\max}	α	x_{opt}	μ_{\max}	α	x_{opt}	μ_{\max}	α	x_{opt}	μ_{\max}	α	x_{opt}	μ_{\max}	α	x_{opt}	μ_{\max}	α	x_{opt}	μ_{\max}	α	x_{opt}	μ_{\max}	α	x_{opt}
μ_{\max}	1.00	-0.30	0.05	1.00	-0.39	-0.07	1.00	-0.47	-0.32	1.00	-0.46	-0.38	1.00	-0.47	-0.39	1.00	-0.50	-0.19	1.00	-0.46	-0.24	1.00	-0.51	-0.30
α	-0.30	1.00	0.53	-0.39	1.00	0.47	-0.47	1.00	0.18	-0.46	1.00	-0.09	-0.47	1.00	0.11	-0.50	1.00	-0.27	-0.46	1.00	-0.23	-0.51	1.00	0.18
x_{opt}	0.05	0.53	1.00	-0.07	0.47	1.00	-0.32	0.18	1.00	-0.38	-0.09	1.00	-0.39	0.11	1.00	-0.19	-0.27	1.00	-0.24	-0.23	1.00	-0.30	0.18	1.00
(5)	γ_{\max}	x^*	γ_{\max}	x^*	γ_{\max}	x^*	γ_{\max}	x^*	γ_{\max}	x^*	γ_{\max}	x^*	γ_{\max}	x^*	γ_{\max}	x^*	γ_{\max}	x^*	γ_{\max}	x^*	γ_{\max}	x^*	γ_{\max}	x^*
γ_{\max}	1.00	-0.81	1.00	-0.78	1.00	-0.39	1.00	-0.07	1.00	-0.18	1.00	-0.05	1.00	-0.14	1.00	-0.14	1.00	-0.14	1.00	-0.14	1.00	-0.48	1.00	-0.48
x^*	-0.81	1.00	-0.78	1.00	-0.39	1.00	-0.07	1.00	-0.18	1.00	-0.05	1.00	-0.14	1.00	-0.14	1.00	-0.14	1.00	-0.14	1.00	-0.48	1.00	-0.48	1.00

Table 2: Correlation matrix of parameter estimation error of five parameterizations (1)-(5) for eight microalgae species (1: *Skeletonema costatum*, 2: *Isochrysis galbana*, 3: *Dunaliella salina*, 4: *Platymonas subcordiformis*, 5: *Chlorococcum sp.* FACHB-1556, 6: *Microcystis aeruginosa* FACHB-905, 7: *Microcystis wesenbergii* FACHB-1112, 8: *Scenedesmus obliquus* FACHB-116). Note that "—" represents the case where the Fisher information matrix F is singular, and we cannot obtain an accurate result.

Andrews (1) are strongly correlated. This is expected since all three parameters are complex combination of the three fundamental parameters, as shown in the previous section. There are only two microalgae species for which we are able to determine the correlation matrix for the parameterization of Edwards (2). This is due to the fact that the related Fisher information matrix F is singular. For these two species, we observe once again a strong correlation between the three parameters (μ_m, K_x, K_i) in (2). This further confirms the identifiability issue reported in [34]. Regarding the parameterization of Peeters (3), there is a strong correlation between the parameters a and b , and both are rather uncorrelated with the parameter c . The correlation coefficient between the parameters assesses whether the parameters are independent. If one of the parameters is not independent, then the correlated parameters are likely to produce similar information, and the parameterization is thus less efficient. Based on our observations, parameterizations of Bernard (4) and KIS (5) are more suitable to represent the growth rate with respect to irradiance for the eight microalgae species.

Best parameterization of the inhibition kinetics

In general, the minimum value of AIC_c or BIC reveals the best trade-off between the number of parameters m and the ability to fit the data among different models. However, this becomes less clear for selecting equivalent parameterizations of one model. Table 3 presents the AIC_c , BIC values as well as the values obtained using the new criterion PEMAC for the five parameterizations (1)-(5) and for eight microalgae species. We observe that the AIC_c and BIC values do not vary significantly among the five parameterizations, especially for the species *Platymonas subcordiformis* and *Chlorococcum sp.* FACHB-1556. Thus, based on the values of AIC_c and BIC , it is less clear which parameterization is better among (1)-(5). This ambiguity disappears when using our new criterion PEMAC. Indeed, there is a clear difference in the PEMAC value between the five parameterizations, even in the case of the species *Platymonas subcordiformis* and *Chlorococcum sp.* FACHB-1556, where the criteria AIC_c and BIC are unable to distinguish. Furthermore, we observe that the parameterization of Bernard (4) has the minimum value of PEMAC most of the time, except for the species *Platymonas subcordiformis* and *Chlorococcum sp.* FACHB-1556, where the parameterization KIS (5) has the minimum PEMAC value. Otherwise, our parameterization KIS is often the second or third best parameterization, meaning that it also provides a good representation of the growth rate with respect to the irradiance using only two parameters. Regarding the parameterization of Edwards (2), we are only able to provide the PEMAC value for two species, as to compute the average error propagation (17), we need the Fisher information matrix F which is unavailable due to the singularity issue. This shows again the accuracy problem of the parameterization of Edwards.

Prediction interval and parameter sensitivity

To further check the quality of using each parameterization μ^k to characterize the growth rate with respect to the irradiance, Fig. A.1 - A.8 show the prediction interval (PI) (12) of each parameterization for all eight microalgae

	(1)	(2)	(3)	(4)	(5)
<i>Skeletonema costatum</i>					
AIC _c	-561.7971	-554.3161	-561.7971	-561.7971	-557.3357
BIC	-559.7858	-552.3049	-559.7858	-559.7858	-555.3959
PEMAC	-928.9370	-	-1028.5730	-1082.4752	-1060.1172
<i>Isochrysis galbana</i>					
AIC _c	-167.2731	-150.9055	-167.2731	-167.2731	-155.2388
BIC	-170.0133	-153.6457	-170.0133	-170.0133	-156.2106
PEMAC	-211.7551	-	-302.2497	-333.9981	-296.7996
<i>Dunaliella salina</i>					
AIC _c	-168.9626	-160.3860	-168.9626	-168.9626	-164.7193
BIC	-171.7028	-163.1262	-171.7028	-171.7028	-165.6911
PEMAC	-287.4636	-	-317.7917	-341.5794	-329.9519
<i>Platymonas subcordiformis</i>					
AIC _c	-150.1121	-150.1121	-150.1121	-150.1121	-149.3011
BIC	-152.8523	-152.8523	-152.8523	-152.8523	-150.2729
PEMAC	-260.5042	-252.3863	-275.0006	-290.3377	-299.8248
<i>Chlorococcum sp.</i> FACHB-1556					
AIC _c	-168.7907	-168.7907	-168.7907	-168.7907	-171.8261
BIC	-171.5309	-171.5309	-171.5309	-171.5309	-172.7979
PEMAC	-295.6872	-275.4283	-314.1104	-333.2404	-348.9473
<i>Microcystis aeruginosa</i> FACHB-905					
AIC _c	-132.6640	-105.0685	-132.6640	-132.6640	-109.7828
BIC	-136.4387	-108.8432	-136.4387	-136.4387	-111.3281
PEMAC	-157.6629	-	-236.6074	-259.9892	-219.0630
<i>Microcystis wesenbergii</i> FACHB-1112					
AIC _c	-153.6035	-126.5084	-153.6035	-153.6035	-130.8417
BIC	-156.3437	-129.2486	-156.3437	-156.3437	-131.8136
PEMAC	-137.3329	-	-279.3771	-302.4023	-262.9083
<i>Scenedesmus obliquus</i> FACHB-116					
AIC _c	-140.6828	-113.2002	-140.6828	-140.6828	-117.9145
BIC	-144.4574	-116.9749	-144.4574	-144.4574	-119.4598
PEMAC	-177.7300	-	-252.0564	-278.5561	-232.4748

Table 3: The AIC_c, BIC and PEMAC values of the parameterizations (1)-(5) for each microalgae species in [35] and [36]

species. For the sake of compactness, these figures are provided in Appendix A. From the scale and shape of the PI, we observe that both parameterizations of Bernard (4) and KIS (5) provide a relatively good prediction compared to the other three parameterizations (1)-(3). And once again, we are only able to show the PI curve of the parameterization of Edwards (2) for the species *Platymonas subcordiformis* and *Chlorococcum sp.* FACHB-1556, this is due to the singularity issue of the Fisher information matrix F for the other species.

In addition, we can also study the parameter sensitivity using the normalized sensitivity (13). Fig. B.9 - B.16 in Appendix B present the normalized sensitivity of each parameterization μ^k with respect to the related parameter set θ^k for the eight microalgae species. For the parameterization of Bernard (4), we observe that the parameter α (red curve) has a strong sensitivity for small irradiance values, since α represents the initial slope of the growth rate curve. Moreover, μ_{\max} (blue curve) is the most sensitive parameter when the irradiance approaches x_{opt} , and the sensitivities of α and x_{opt} (yellow curve) go to zero. This is related to the partial derivatives $\frac{\partial \mu^1}{\partial \theta_j^1}$. Indeed, when x approaches x_{opt} , the partial derivatives $\frac{\partial \mu^1}{\partial \alpha}$, $\frac{\partial \mu^1}{\partial x_{\text{opt}}}$ are both close to 0 and $\frac{\partial \mu^1}{\partial \mu_{\max}}$ is close to 1. Thus, μ_{\max} is the most sensitive parameter around x_{opt} . When moving to large values of irradiance, we observe that x_{opt} becomes more sensitive than the other two parameters.

Concerning the parameterizations of Andrews (1) and Edwards (2), we observe that the parameter $\bar{\mu}$ (blue curve) is relatively sensitive along with the irradiance, the sensitivity of the parameter K_x (red curve) decreases as the irradiance increases, and the sensitivity of the parameter K_i (yellow curve) increases as the irradiance decreases, which is in line with the structure of this parameterization, where K_x dominates the numerator at low light and x^2/K_i at high light.

For the parameterization of Peeters (3), we observe that the parameter c (yellow curve) is relatively sensitive only for small irradiance values, the sensitivity of the parameter a (blue curve) increases as the irradiance increases, and the sensitivity curve of the parameter b (red curve) shares the same shape as the growth rate. Recall that the parameter c is related to the initial slope of the growth rate, which explains its sensitivity only for small irradiance values.

Regarding our parameterization KIS (5), we observe that the sensitivity curves of the parameters γ_{\max} and x^* are rather symmetric, with a horizontal symmetrical axis at 0.5. The parameter x^* represents the value for

which growth is maximum, and γ_{\max} is proportional to the maximum growth rate. The roles of both parameters are well-balanced, and they share equally the task of representing the growth rate with respect to the irradiance. Moreover, we find that α in the parameterization of Bernard (4) is only sensitive for small irradiance, μ_{\max} and x_{opt} rather dominate separately for the rest part. This actually confirms the behavior of our parameterization, as γ_{\max} is very related to μ_{\max} and x^* to x_{opt} . By well choosing these two parameters using their equivalent relationship, our parameterization (5) can very efficiently capture the growth rate.

Conclusion

In this study, we have reviewed and examined four parameterizations (1)-(4) of the Haldane model existing in the literature. We have also introduced a new parameterization KIS (5) based on only two parameters. The parameterization of Edwards (2), even if it has been used in the literature, has identifiability problems that lead to disastrous numerical consequences. The parameterizations of Andrews (1) and Peeters (3) exhibit a strong correlation between the parameters and the subsequent poor prediction accuracy. The parameterization of Bernard (4), which efficiently uncorrelates the three parameters, is the most efficient representation with three parameters. Surprisingly, our two-parameter parameterization KIS (5) out-competes all the other models.

This conclusion on the capability of the parameterization KIS (5) to accurately represent the inhibition of photosynthetic organisms by high light would need to be verified with other cases of growth inhibition (volatile fatty acids, ethanol, phenol, etc.). It perfectly illustrates the principle of "Keep It Simple (KIS)", which should guide the modelling [34]. With fewer parameters, the identification procedure is more efficient, and eventually the modelling uncertainty is better contained than a more complex model, which pay the price of having more parameters.

References

- [1] Spolaore P, Joannis-Cassan C, Duran E, Isambert A. Commercial applications of microalgae. *Journal of Bioscience and Bioengineering*. 2006;101(2):87–96. doi:10.1263/jbb.101.87.
- [2] Becker EW. Micro-algae as a source of protein. *Biotechnology Advances*. 2007;25(2):207–210. doi:10.1016/j.biotechadv.2006.11.002.
- [3] Kent M, Welladsen HM, Mangott A, Li Y. Nutritional Evaluation of Australian Microalgae as Potential Human Health Supplements. *PLOS ONE*. 2015;10(2):1–14. doi:10.1371/journal.pone.0118985.
- [4] Wang Y, Tibbetts SM, McGinn PJ. Microalgae as Sources of High-Quality Protein for Human Food and Protein Supplements. *Foods*. 2021;10(12). doi:10.3390/foods10123002.
- [5] Jagadevan S, Banerjee A, Banerjee C, Guria C, Tiwari R, Baweja M, et al. Recent developments in synthetic biology and metabolic engineering in microalgae towards biofuel production. *Biotechnol Biofuels*. 2018;11. doi:10.1186/s13068-018-1181-1.
- [6] Mata TM, Martins AA, Caetano NS. Microalgae for biodiesel production and other applications: A review. *Renewable and Sustainable Energy Reviews*. 2010;14(1):217–232. doi:10.1016/j.rser.2009.07.020.
- [7] Zibarev N, Toumi A, Politaeva N, Iljin I. Nutrients recovery from dairy wastewater by Chlorella vulgaris and comparison of the lipid's composition with various chlorella strains for biodiesel production. *PLOS ONE*. 2024;19(4):1–13. doi:10.1371/journal.pone.0297464.
- [8] Taher H, Al-Zuhair S, Al-Marzouqi A, Haik Y, Farid M. Growth of microalgae using CO₂ enriched air for biodiesel production in supercritical CO₂. *Renewable Energy*. 2015;82:61–70. doi:10.1016/j.renene.2014.08.013.
- [9] Arora AS, Nawaz A, Qyyum MA, Ismail S, Aslam M, Tawfik A, et al. Energy saving anammox technology-based nitrogen removal and bioenergy recovery from wastewater: Inhibition mechanisms, state-of-the-art control strategies, and prospects. *Renewable and Sustainable Energy Reviews*. 2021;135:110126.
- [10] Edwards VH. The influence of high substrate concentrations on microbial kinetics. *Biotechnology and Bioengineering*. 1970;12(5):679–712. doi:10.1002/bit.260120504.

- [11] Bernard O, Rémond B. Validation of a simple model accounting for light and temperature effect on microalgal growth. *Bioresource Technology*. 2012;123:520–527. doi:10.1016/j.biortech.2012.07.022.
- [12] Ucun H, Yildiz E, Nuhoglu A. Phenol biodegradation in a batch jet loop bioreactor (JLB): Kinetics study and pH variation. *Bioresource Technology*. 2010;101(9):2965–2971.
- [13] Jimenez J, Latrille E, Harmand J, Robles A, Ferrer J, Gaida D, et al. Instrumentation and control of anaerobic digestion processes: a review and some research challenges. *Reviews in Environmental Science and Bio/Technology*. 2015;14:615–648.
- [14] Bernard O, Lu LD. Optimal optical conditions for Microalgal production in photobioreactors. *Journal of Process Control*. 2022;112:69–77. doi:10.1016/j.jprocont.2022.03.001.
- [15] Lee E, Jalalizadeh M, Zhang Q. Growth kinetic models for microalgae cultivation: A review. *Algal Research*. 2015;12:497–512. doi:10.1016/j.algal.2015.10.004.
- [16] Monod J. Recherches sur la croissance des cultures bactériennes. Université de Paris. Paris; 1941.
- [17] Jannasch HW, Egli T. Microbial growth kinetics: a historical perspective. *Antonie van Leeuwenhoek*. 1993;63:213–224. doi:10.1007/BF00871219.
- [18] Hsu SB, Waltman P. A survey of mathematical models of competition with an inhibitor. *Mathematical Biosciences*. 2004;187(1):53–91. doi:10.1016/j.mbs.2003.07.004.
- [19] Andrews JF. A mathematical model for the continuous culture of microorganisms utilizing inhibitory substrates. *Biotechnology and Bioengineering*. 1968;10(6):707–723. doi:10.1002/bit.260100602.
- [20] Haldane JBS. Enzymes. London: Longmans, Green & Co.; 1930.
- [21] D'Adamo PD, Rozich AF, Jr AFG. Analysis of Growth Data with Inhibitory Carbon Sources. *Biotechnology and Bioengineering*. 1984;26:397–402. doi:10.1002/bit.260260421.
- [22] Han K, Levenspiel O. Extended Monod Kinetics for Substrate, Product, and Cell Inhibition. *Biotechnology and Bioengineering*. 1988;32:430–437. doi:10.1002/bit.260320404.
- [23] Reardon KF, Mosteller DC, Bull Rogers JD. Biodegradation kinetics of benzene, toluene, and phenol as single and mixed substrates for *Pseudomonas putida* F1. *Biotechnology and Bioengineering*. 2000;69(4):385–400. doi:10.1002/1097-0290(20000820)69:4<385::AID-BIT5>3.0.CO;2-Q.
- [24] Banerjee A, Ghoshal AK. Phenol degradation by *Bacillus cereus*: pathway and kinetic modeling. *Bioresource Technology*. 2010;101(14):5501–5507.
- [25] García-Díéguez C, Bernard O, Roca E. Reducing the Anaerobic Digestion Model No. 1 for its application to an industrial wastewater treatment plant treating winery effluent wastewater. *Bioresource technology*. 2013;132:244–253.
- [26] Kok B. On the inhibition of photosynthesis by intense light. *Biochimica et Biophysica Acta*. 1956;21(2):234–244. doi:10.1016/0006-3002(56)90003-8.
- [27] Peeters JCH, Eilers PHC. The relationship between light intensity and photosynthesis—A simple mathematical model. *Hydrobiological Bulletin*. 1978;12(2):134–136. doi:10.1007/BF02260714.
- [28] Growth kinetics of photosynthetic microorganisms. vol. 23. Springer Berlin Heidelberg; 1982.
- [29] Eilers PHC, Peeters JCH. A model for the relationship between light intensity and the rate of photosynthesis in phytoplankton. *Ecological Modelling*. 1988;42:199–215. doi:10.1016/0304-3800(88)90057-9.
- [30] Talbot P, Thébault JM, Dauta A, Noüe* JDL. A comparative study and mathematical modeling of temperature, light and growth of three microalgae potentially useful for wastewater treatment. *Water Research*. 1991;25(4):465–472. doi:10.1016/0043-1354(91)90083-3.
- [31] Hill GA, Robinson CW. Substrate inhibition kinetics: phenol degradation by *Pseudomonas putida*. *Biotechnology and Bioengineering*. 1975;17(11):1599–1615. doi:10.1002/bit.260171105.

- [32] Wang SJ, Loh KC. Modeling the role of metabolic intermediates in kinetics of phenol biodegradation. *Enzyme and Microbial Technology*. 1999;25(3-5):177–184. doi:10.1016/S0141-0229(99)00060-5.
- [33] Boon B, Laudelout H. Kinetics of Nitrite Oxidation by *Nitrobacter winogradskyi*. *Biochemical Journal*. 1962;85(3):440–447. doi:10.1042/bj0850440.
- [34] Mairet F, Bernard O. Twelve quick tips for designing sound dynamical models for bioprocesses. *PLoS Computational Biology*. 2019;15(8):e1007222.
- [35] Anning T, MacIntyre HL, Pratt SM, Sammes PJ, Gibb S, Geider RJ. Photoacclimation in the marine diatom *Skeletonema costatum*. *Limnology and Oceanography*. 2000;45(8):1807–1817. doi:10.4319/lo.2000.45.8.1807.
- [36] Yang XL, Liu LH, Yin ZK, Wang XY, Wang SB, Ye ZP. Quantifying photosynthetic performance of phytoplankton based on photosynthesis–irradiance response models. *Environmental sciences Europe*. 2020;32(1). doi:10.1186/s12302-020-00306-9.
- [37] James G, Witten D, Hastie T, Tibshirani R. *An introduction to statistical learning*. Springer; 2013.
- [38] Chatterjee S, Hadi AS. *Regression Analysis by Example*. Wiley Series in Probability and Statistics. Wiley; 2006.
- [39] Lagarias JC, Reeds JA, Wright MH, Wright PE. Convergence properties of the Nelder–Mead simplex method in low dimensions. *SIAM Journal on optimization*. 1998;9(1):112–147.
- [40] van Impe JF, Vanrolleghem PA, Iserentant DM, editors. *Advanced Instrumentation, Data Interpretation, and Control of Biotechnological Processes*. Springer Netherlands; 1998.
- [41] Casagli F, Rossi S, Steyer JP, Bernard O, Ficara E. Balancing microalgae and nitrifiers for wastewater treatment: can inorganic carbon limitation cause an environmental threat? *Environmental science & technology*. 2021;55(6):3940–3955.
- [42] Cariboni J, Gatelli D, Liska R, Saltelli A. The role of sensitivity analysis in ecological modelling. *Ecological Modelling*. 2007;203(1):167–182. doi:10.1016/j.ecolmodel.2005.10.045.
- [43] Kenneth PB, David RA, editors. *Model Selection and Multimodel Inference*. Springer-Verlag New York; 1998.
- [44] Burnham KP, Anderson DR, P HK. AIC model selection and multimodel inference in behavioral ecology: some background, observations, and comparisons. *Behavioral ecology and sociobiology*. 2011;65(1):23–35.
- [45] McQuarrie ADR, Tsai CL. *Regression and Time Series Model Selection*. World Scientific; 1998.
- [46] Burnham KP, Anderson DR. Multimodel Inference: Understanding AIC and BIC in Model Selection. *Sociological Methods and Research*. 2004;33(2):261–304.

S1 Appendix: Prediction intervals

We present the prediction intervals of the five parameterizations (1)-(5) for each microalgae species. For all figures, the blue points represent the experimental data obtained from [35, 36], the red line is the fitted curve using the optimal parameter values obtained in Table 1. The purple (resp. yellow) dashed line is the upper (resp. lower) bound of the prediction interval computed using (12). Note that we can only find prediction intervals for four parameterizations in some tested cases, as the Fisher information matrix for the parameterization of Edwards (2) is singular. Hence, we cannot compute e in (12) in these cases. Recall also that Z is the value in the two-tailed Student's t -table. For the experimental data in [35, 36], when the size of samples n is 12, $Z = 2.201$, $Z = 2.179$ when $n = 13$, and $Z = 2.080$ when $n = 22$.

Skeletonema costatum

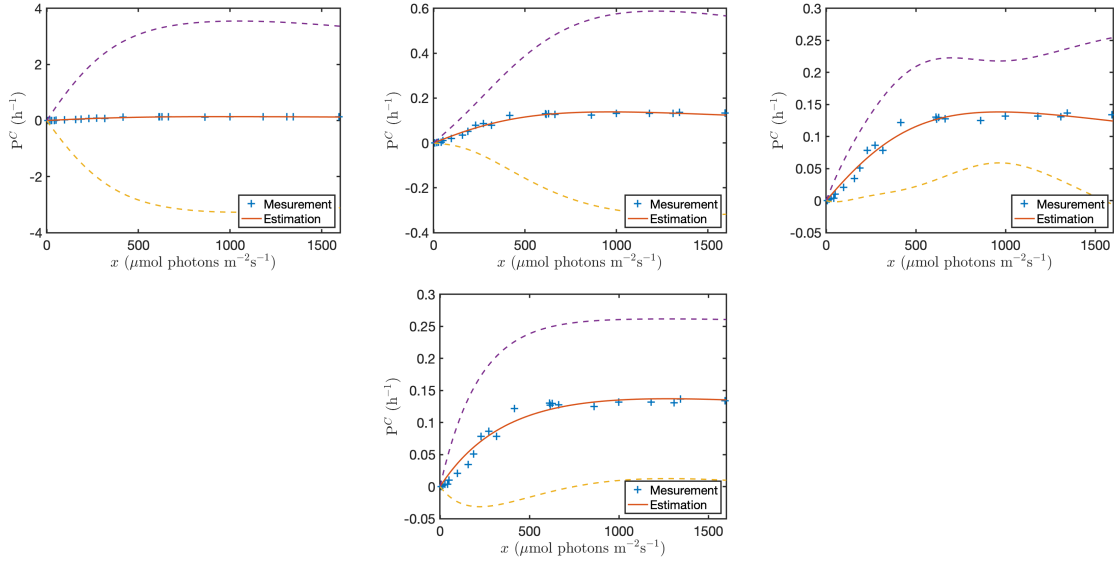


Figure 2: Prediction intervals of four parameterizations with respect to the irradiance x for the experimental data of *Skeletonema costatum* [35]. Top left: Andrews (1). Top middle: Peeters and Eilers (3). Top right: Bernard and Rémond (4). Bottom: KIS (5).

Isochrysis galbana

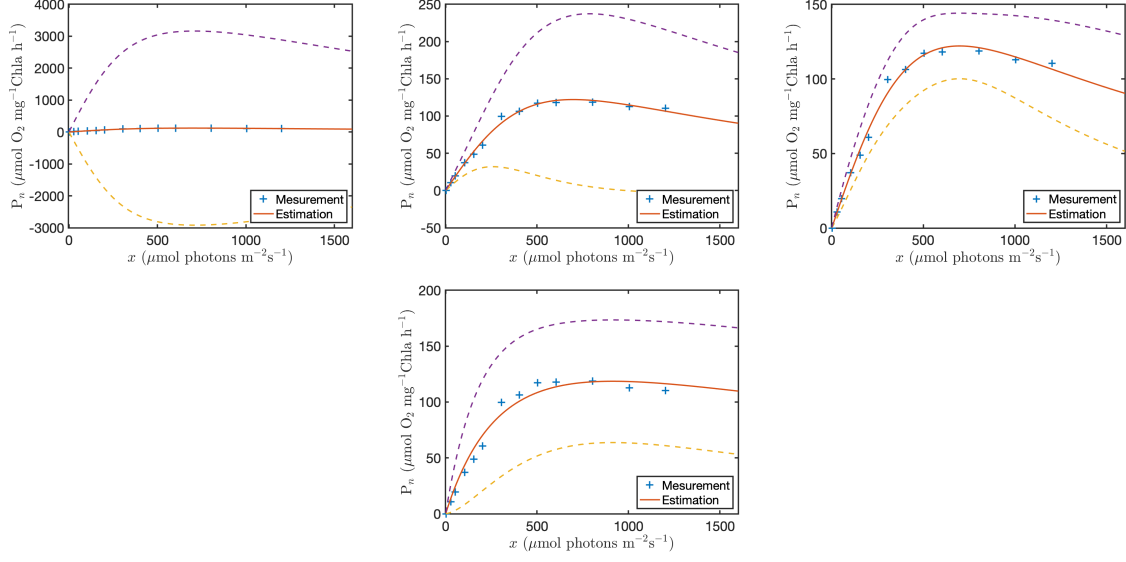


Figure 3: Prediction intervals of four parameterizations with respect to the irradiance x for the experimental data of *Isochrysis galbana* [36]. Top left: Andrews (1). Top middle: Peeters and Eilers (3). Top right: Bernard and Rémond (4). Bottom: KIS (5).

Dunaliella salina

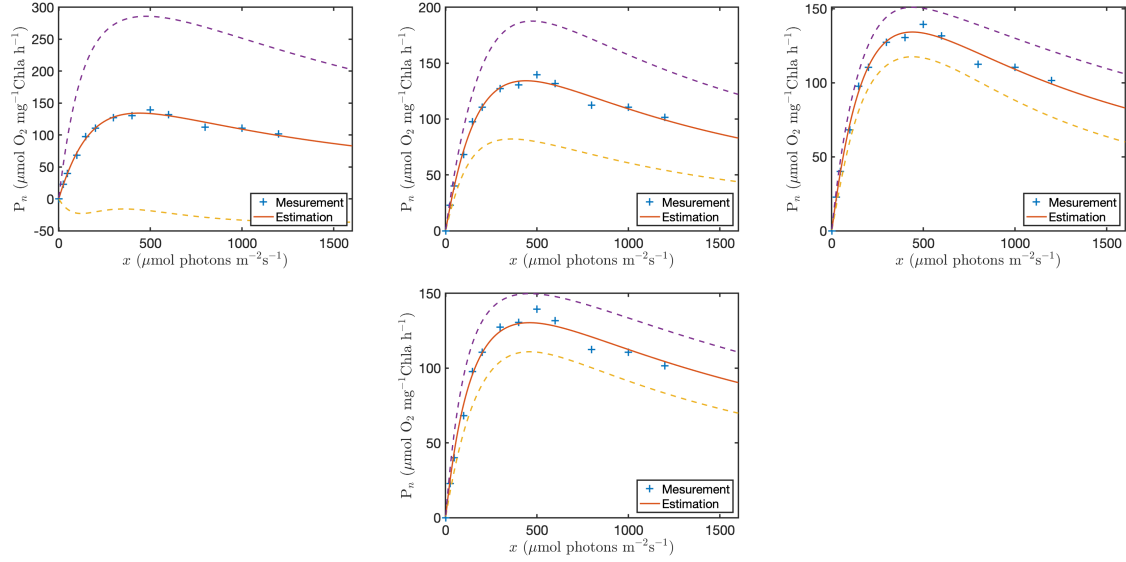


Figure 4: Prediction intervals of four parameterizations with respect to the irradiance x for the experimental data of *Dunaliella salina* [36]. Top left: Andrews (1). Top middle: Peeters and Eilers (3). Top right: Bernard and Rémond (4). Bottom: KIS (5).

Platymonas subcordiformis

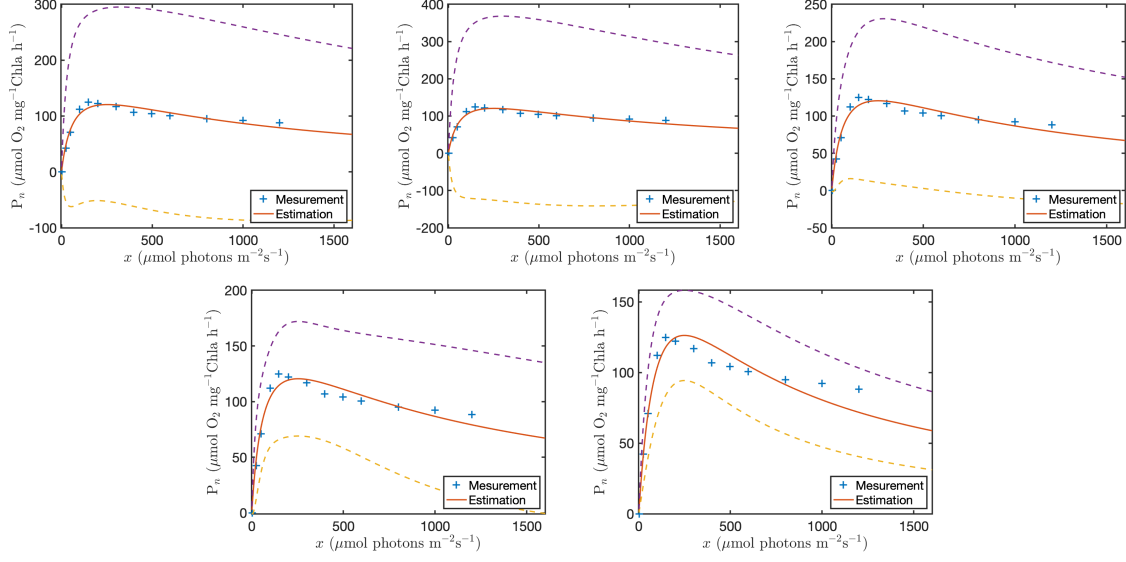


Figure 5: Prediction intervals of five parameterizations with respect to the irradiance x for the experimental data of *Platymonas subcordiformis* [36]. Top left: Andrew (1). Top middle: Edwards (2). Top right: Peeters and Eilers (3). Bottom left: Bernard and Rémond (4). Bottom right: KIS (5).

Chlorococcum sp. FACHB-1556

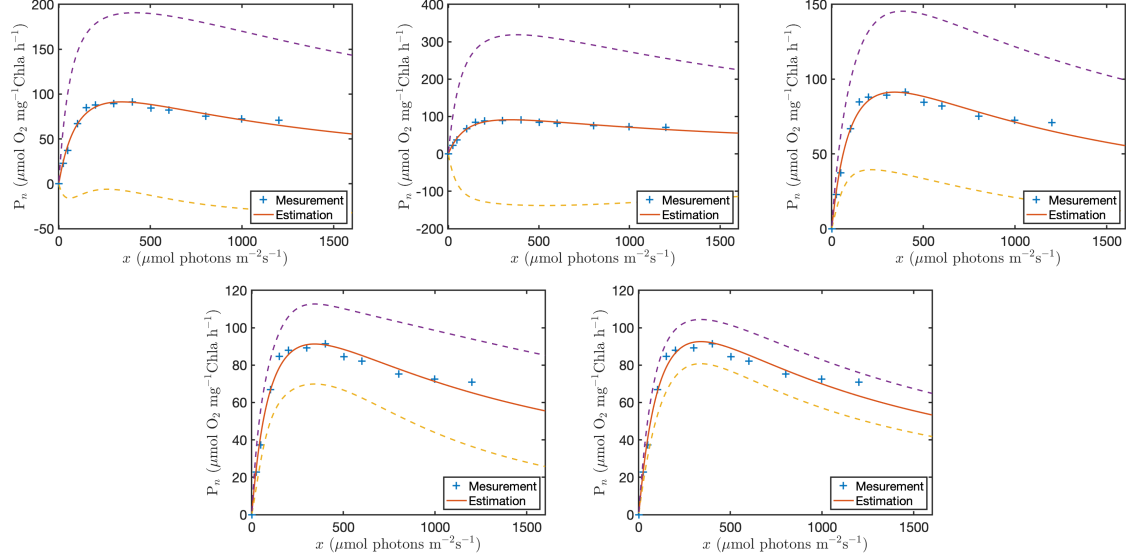


Figure 6: Prediction intervals of five parameterizations with respect to the irradiance for the experimental data of *Chlorococcum sp.* FACHB-1556 [36]. Top left: Andrew (1). Top middle: Edwards (2). Top right: Peeters and Eilers (3). Bottom left: Bernard and Rémond (4). Bottom right: KIS (5).

Microcystis aeruginosa FACHB-905

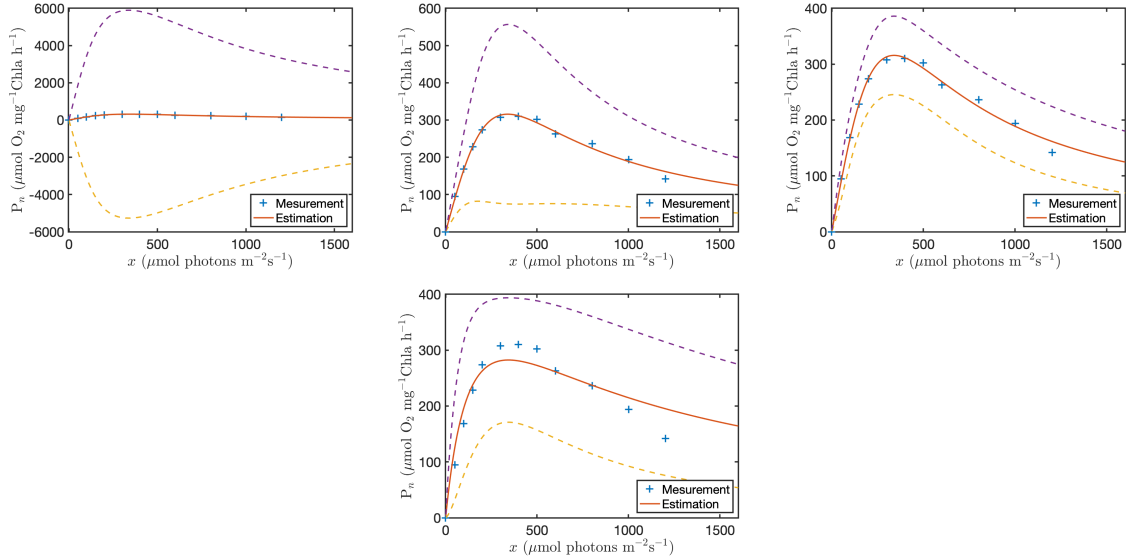


Figure 7: Prediction intervals of four parameterizations with respect to the irradiance x for the experimental data of *Microcystis aeruginosa* FACHB-905 [36]. TTop left: Andrews (1). Top middle: Peeters and Eilers (3). Top right: Bernard and Rémond (4). Bottom: KIS (5).

Microcystis wesenbergii FACHB-1112

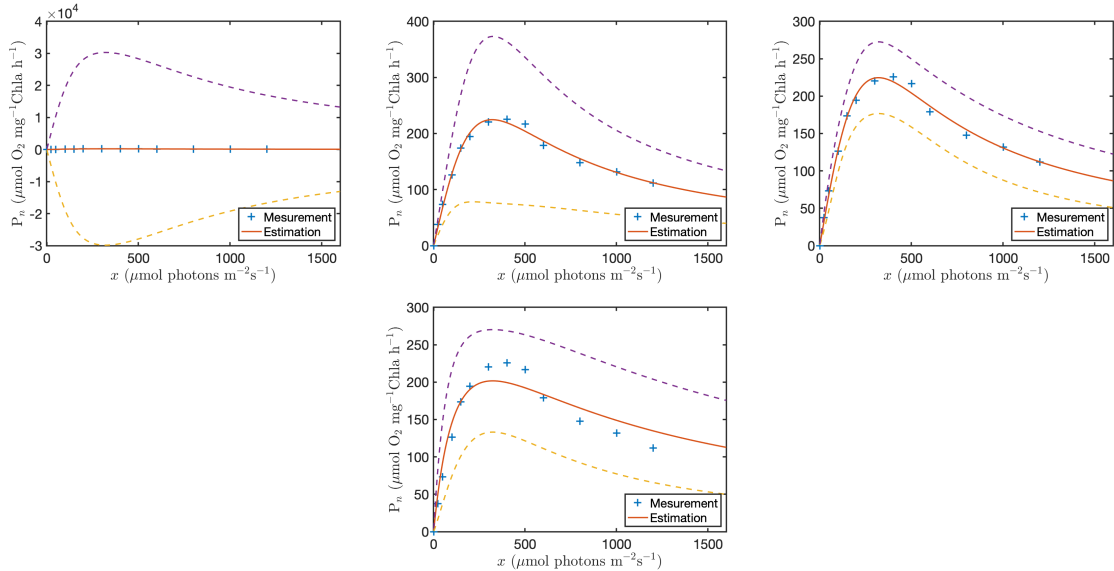


Figure 8: Prediction intervals of four parameterizations with respect to the irradiance x for the experimental data of *Microcystis wesenbergii* FACHB-1112 [36]. Top left: Andrews (1). Top middle: Peeters and Eilers (3). Top right: Bernard and Rémond (4). Bottom: KIS (5).

Scenedesmus obliquus FACHB-116

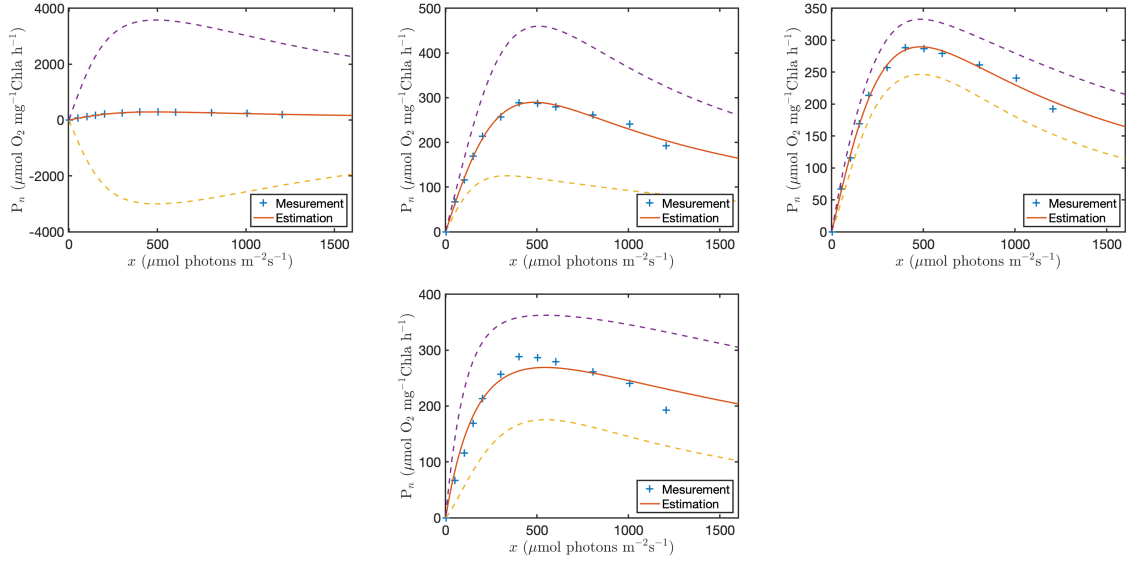


Figure 9: Prediction intervals of four parameterizations with respect to the irradiance x for the experimental data of *Scenedesmus obliquus* FACHB-116 [36]. Top left: Andrews (1). Top middle: Peeters and Eilers (3). Top right: Bernard and Rémond (4). Bottom: KIS (5).

S2 Appendix: Normalized sensitivity

We present here the normalized sensitivity of all five parameterizations (1)-(5) for each microalgae species using (13). Once again, we cannot present the results of the parameterization of Edwards (2) in some cases, as the Fisher information matrix is singular.

Skeletonema costatum

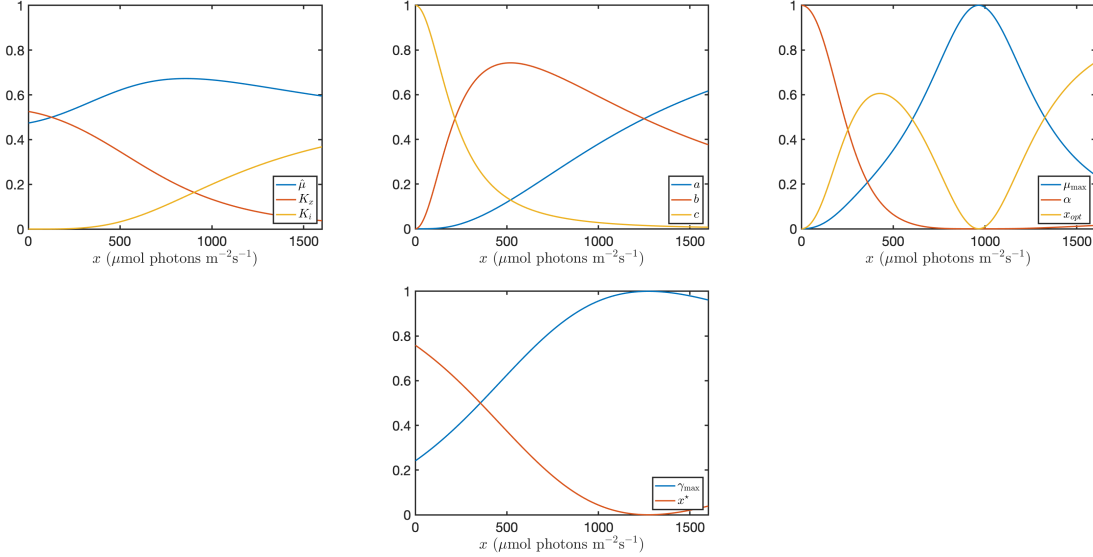


Figure 10: Normalized sensitivity for each parameter of four parameterizations with respect to the irradiance x for the experimental data of *Skeletonema costatum* [35]. Top left: Andrews (1). Top middle: Peeters and Eilers (3). Top right: Bernard and Rémond (4). Bottom: KIS (5).

Isochrysis galbana

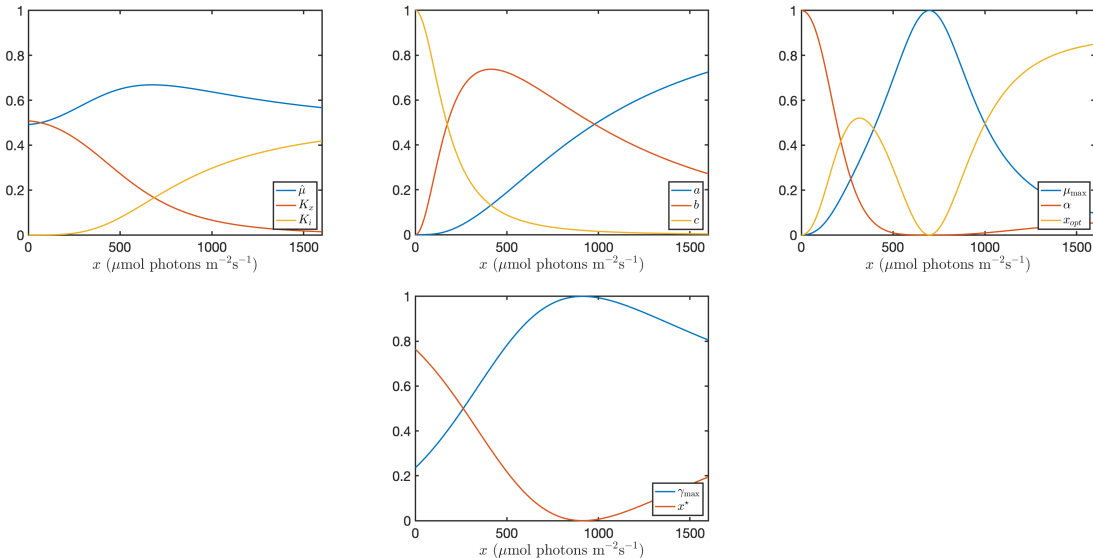


Figure 11: Normalized sensitivity for each parameter of four parameterizations with respect to the irradiance x for the experimental data of *Isochrysis galbana* [36]. Top left: Andrews (1). Top middle: Peeters and Eilers (3). Top right: Bernard and Rémond (4). Bottom: KIS (5).

Dunaliella salina

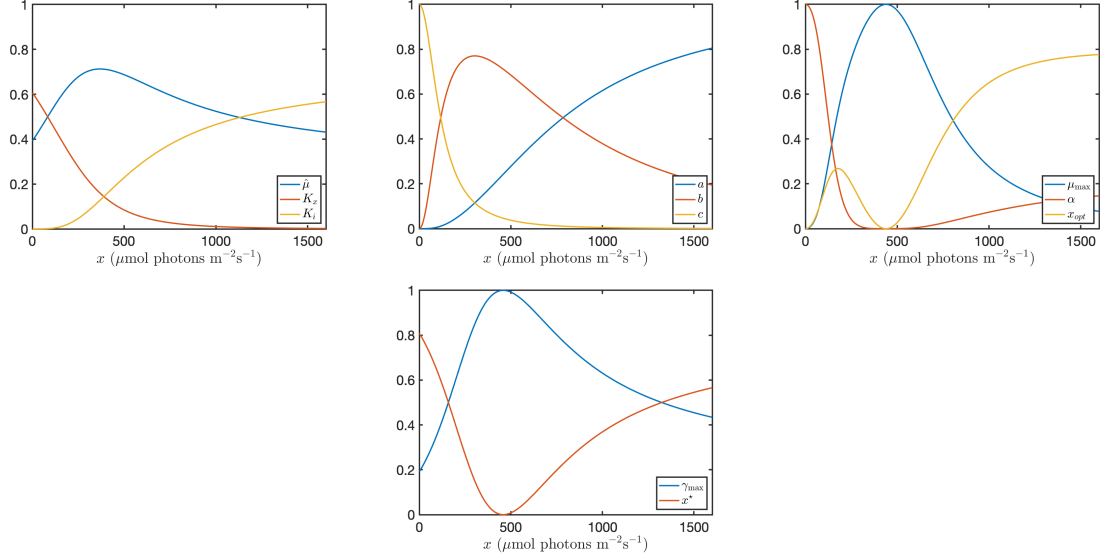


Figure 12: Normalized sensitivity for each parameter of four parameterizations with respect to the irradiance x for the experimental data of *Dunaliella salina* [36]. Top left: Andrews (1). Top middle: Peeters and Eilers (3). Top right: Bernard and Rémond (4). Bottom: KIS (5).

Platymonas subcordiformis

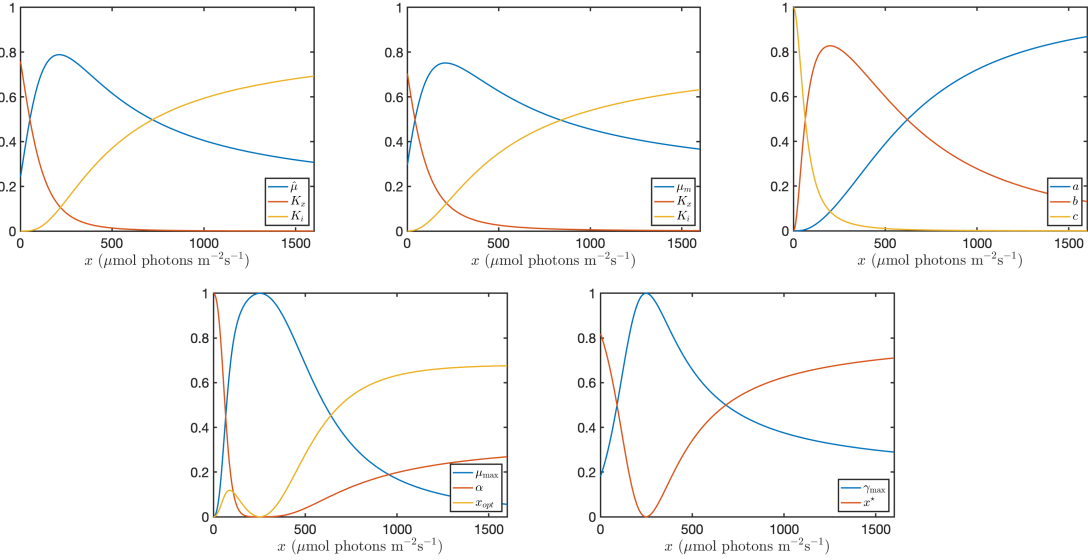


Figure 13: Normalized sensitivity for each parameter of five parameterizations with respect to the irradiance x for the experimental data of *Platymonas subcordiformis* [36]. Top left: Andrew (1). Top middle: Edwards (2). Top right: Peeters and Eilers (3). Bottom left: Bernard and Rémond (4). Bottom right: KIS (5).

Chlorococcum sp. FACHB-1556

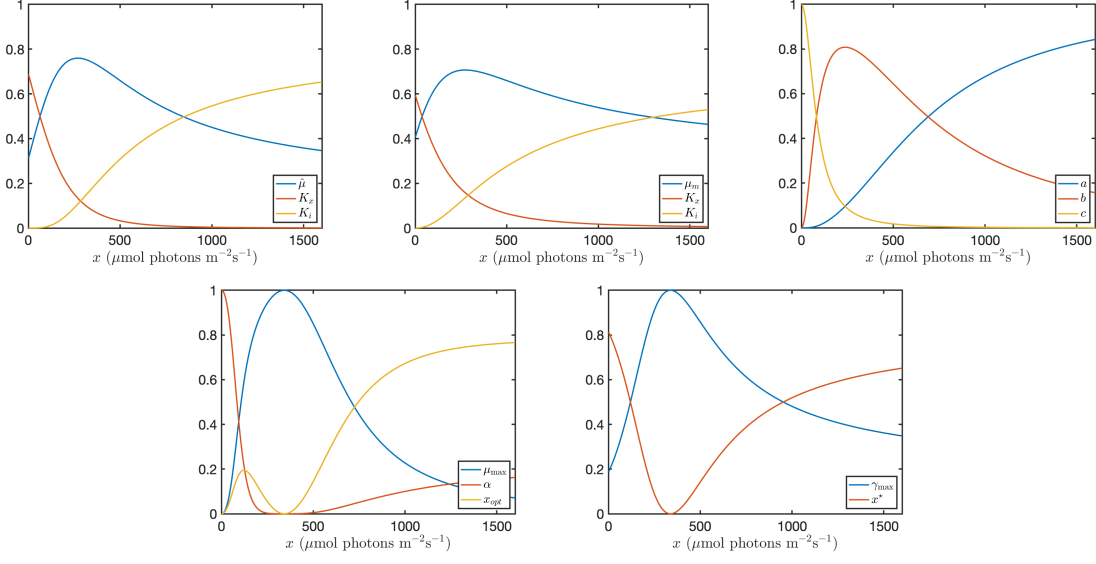


Figure 14: Normalized sensitivity for each parameter of five parameterizations with respect to the irradiance x for the experimental data of *Chlorococcum* sp. FACHB-1556 [36]. Top left: Andrew (1). Top middle: Edwards (2). Top right: Peeters and Eilers (3). Bottom left: Bernard and Rémond (4). Bottom right: KIS (5).

Microcystis aeruginosa FACHB-905

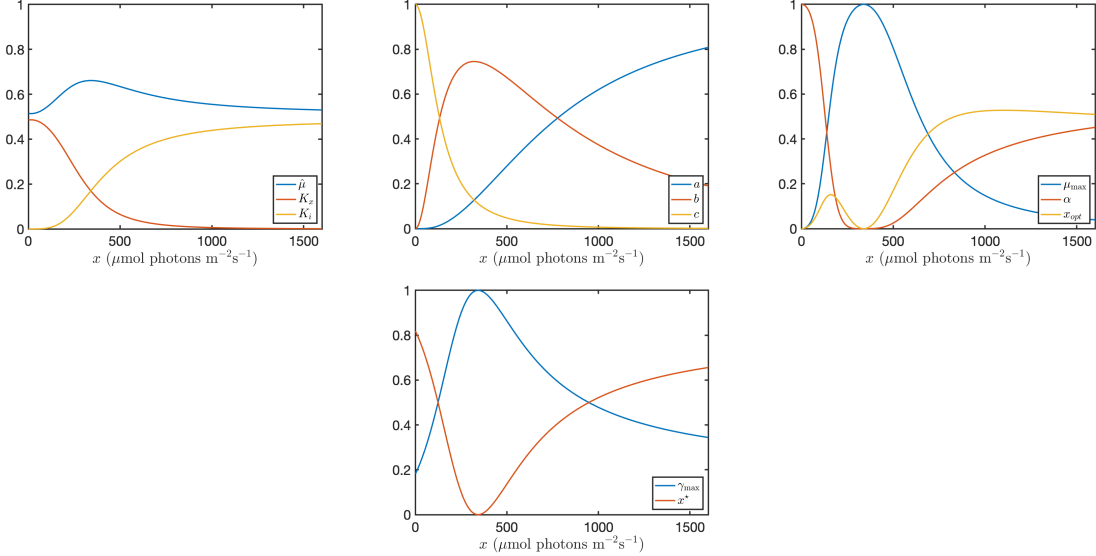


Figure 15: Normalized sensitivity for each parameter of four parameterizations with respect to the irradiance x for the experimental data of *Microcystis aeruginosa* FACHB-905 [36]. Top left: Andrews (1). Top middle: Peeters and Eilers (3). Top right: Bernard and Rémond (4). Bottom: KIS (5).

Microcystis wesenbergii FACHB-1112

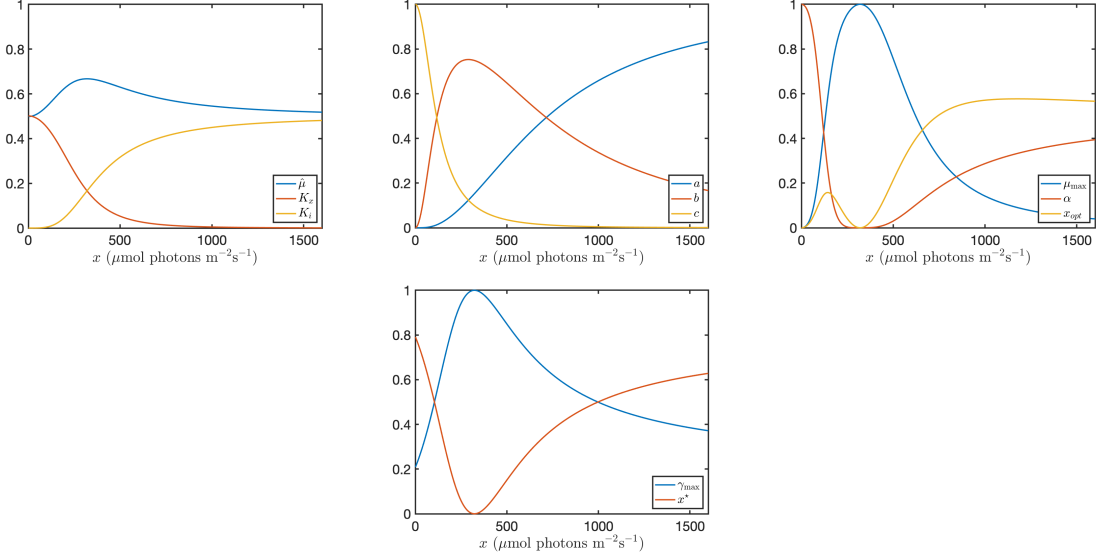


Figure 16: Normalized sensitivity for each parameter of four parameterizations with respect to the irradiance x for the experimental data of *Microcystis wesenbergii* FACHB-1112 [36]. Top left: Andrews (1). Top middle: Peeters and Eilers (3). Top right: Bernard and Rémond (4). Bottom: KIS (5).

Scenedesmus obliquus FACHB-116

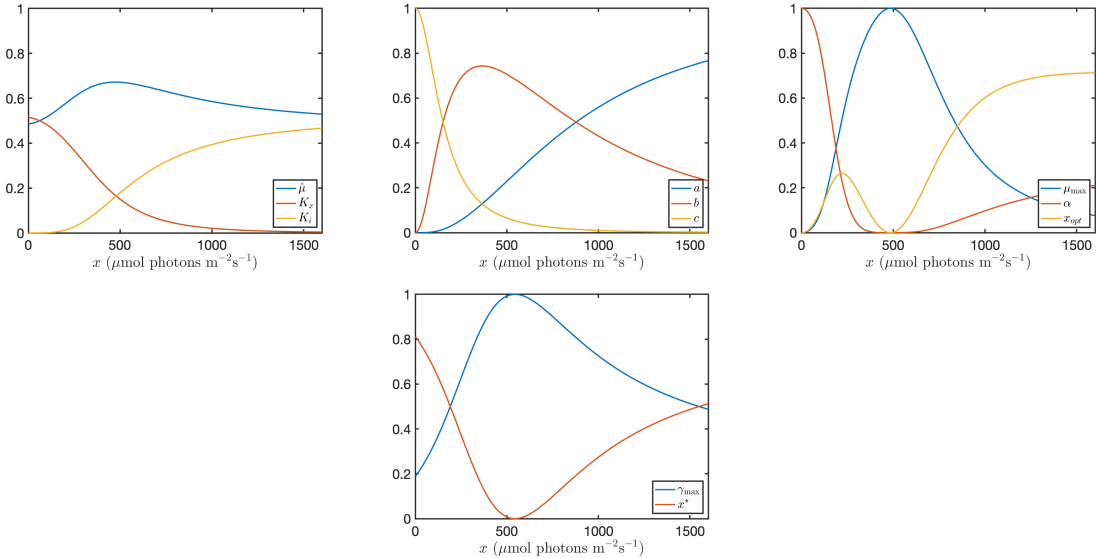


Figure 17: Normalized sensitivity for each parameter of four parameterizations with respect to the irradiance x for the experimental data of *Scenedesmus obliquus* FACHB-116 [36]. Top left: Andrews (1). Top middle: Peeters and Eilers (3). Top right: Bernard and Rémond (4). Bottom: KIS (5).